CHALMERS

Modeling of high-speed data link for wireless communication on ship platform

Master's Thesis in the Communication Engineering

HAO XIE

Department of Signals and Systems
Communication Systems Group
Chalmers University of Technology
Gothenburg, Sweden, 2013
Master's Thesis 2013

Modeling of high-speed data link for wireless communication on ship platform
NAME HAO XIE

Technical report No. EX041/2013
Department of Signals and Systems
Chalmers University of Technology
SE-412 96 Gothenburg
Sweden
Telephone + 46 (0)31-772 1000

Notation

SPCS	ships platform communication system
EMI	electromagnetic interference
IEMIs	intentional electromagnetic interference
DSSS	direct-sequence spread spectrum
FHSS	frequency-hopping spread spectrum
BER	bit error rate
CRC	cyclic redundancy check
RS	Reed–Solomon
JTIDS	Joint Tactical Information Distribution System
PN	pseudonoise
SNR	signal to noise ratio
SIR	signal to interference ratio
PSD	power spectral density
AWGN	additive white Gaussian noise
BPSK	binary phase-shift keying
FSK	frequency-shift keying
ADS	Advanced Design System

Abstract

Ship platform communication systems (SPCS) are very important for the security of ships on the sea. The SPCS should have good ability to resist electromagnetic interference (EMI), so it is important to explore effective techniques to suppress EMI effects on the wireless communication performance of such ship platforms. Furthermore, it is important to investigate the effect of different kinds of EMI on the SPCS.

In this thesis, an SPCS simulation model has been built, based on direct-sequence spread spectrum (DSSS), frequency-hopping spread spectrum (FHSS) and channel coding technologies. The simulator has been used to investigate the resistance of the SPCS system to various EMI signals.

Key words: SPCS, Direct-sequence spread spectrum (DSSS), Frequency-hopping spread spectrum (FHSS), Electromagnetic interference (EMI), Bit error rate (BER)

Acknowledgements

This M.Sc thesis project has been performed as collaboration between Zhejiang University, China and China Ship Development and Design Center.

I would like to show my gratitude to my supervisor Prof. Wen-yan Yin from Zhejiang University, who has provided me with support, advice and guidance throughout the whole thesis project. And I would also like to thank my examiner Associate Prof. Tommy Svensson from Chalmers University of Technology, who is very patient to answer my questions and thesis process report.

Hao XIE, Gothenburg
19/8/2013

Contents

1 Introduction

The objective of a communication system is to transmit the information from transmitter to receiver correctly. Communication systems on ship platforms always face with a severe transmission environment on the sea and non-intentional or intentional electromagnetic interference (IEMIs) [1][2]. Spread spectrum [3] is the main technology to suppress EMI effects, and channel coding can improve the system performance efficiently.

1.1 Background

With the development of wireless communication technology, high-speed data links become more and more significant in modern communication systems. Much more information can be transmitted at the same time through a high-speed data link, especially for the communication system on ship platforms, where high speed and transmission accuracy are both important. However, communication systems on ship platforms always face with a severe transmission environment on the sea and IEMIs signals, which may degrade the transmission data quality seriously. So a good data link that can resist the severe environment and EMI signals is very significant. Under such circumstances, it will be very important to explore some effective techniques to suppress (I) EMI effects on the wireless communication performance. Spread spectrum is the main technology to suppress EMI effects. In this thesis, the spread spectrum technologies of DSSS and FHSS are used. In addition, channel coding techniques consisting of cyclic redundancy check (CRC), Reed-Solomon (RS) codes and interleaving are also used to improve the communication system performance.

1.2 Goal of this thesis

In this thesis, we have completed the following objectives.

1. To build up a high-speed data link communication system model for ship platforms.
2. With the help of some commercial software, such as MATLAB and Advanced Design System (ADS) etc., to further carry out simulation for predicting the system receiving characteristics.
3. To explore some techniques to suppress electromagnetic interference (EMI) effects on the wireless communication performance.

1.3 Structure

Chapter 2 introduces the high-speed data link for ship platform communication system that we designed in this thesis. Chapter 3 demonstrates the key technologies we used in the SPCS to improve the system performance, such as spread spectrum and channel coding technologies. Chapter 4 describes the EMI signals, and show the built simulation model, time domain waveform and frequency spectrogram of these EMI signals. Chapter 5 presents the simulation results of both software ADS and Simulink. The EMI signals built in chapter 4 are introduced into the simulation model. Then we investigate the system performance of resisting EMI signals. Chapter 6 concludes the whole work of this thesis and states the future work.

2 Ship platform communication system (SPCS)

The high-speed data link for wireless communication we designed is applied on the ship platform with the Link-16/ Joint Tactical Information Distribution System (JTIDS) [4] as a reference in this thesis. This SPCS is used for the communication between ships and control centers. It is also used for the communication between ships. As we know, high speed of the communication system used on the ship platforms is very important, which can ensure the security of ships sailing on the sea. But because of the severe environment on the sea and the existence of some EMI signals, the data link communication system performance of resisting the severe transmission environment and EMI signals is much more important. So the SPCS we designed should ensure normal communication even when the severe sea environment and EMI signals both exist.

In order to improve the SPCS performance of resisting severe transmission environment on the sea and EMI signals, some key technologies of spread spectrum and channel coding are applied, such as DSSS, FHSS, CRC, RS and interleaving. These technologies used in the data link communication system can not only improve the system performance effectively and decrease the system bit error rate (BER), but also make the SPCS to meet the demand of normal communication even when severe sea environment and EMI signals both exist.

3 Key technologies of SPCS

It is very important to explore some effective techniques to suppress (I)EMI effects on the SPCS. In this chapter, we introduce some key technologies to resist severe transmission environment on the sea and EMI signals.

3.1 Spread spectrum

Spread spectrum [3][5] technologies are methods to spread a transmitted signal to a wide frequency band. The spread bandwidth is much wider than the original signal bandwidth. At the receiver, the signal is restored to its original signal bandwidth by using correlative reception. This communication system is named spread spectrum system. There are many merits of spread spectrum communication system, such as high anti-jamming capability to active interference, natural interference and noise, and good security to transmitted information [5]. So spread spectrum technologies are widely used in communication system nowadays.

3.1.1 Theory of spread spectrum

The fundamental theory of spread spectrum can be expressed by the Shannon–Hartley theorem [7] as follows.

$$C = B\log_2(1+S/N)$$

$$= B\log_2(1+S/n_0B) \tag{3.1}$$

where C is channel capacity, S is received signal average power, N is noise power, B is signal bandwidth and n_0 is power spectral density of white noise.

Channel capacity [7] is the highest data rate that information can be transmitted over a communication channel inerrably. In order to transmit information faster, we need to increase the channel capacity. From Eq.(3.1), we can see that bigger channel capacity can be achieved by increasing the signal to noise ratio (SNR) or signal bandwidth B. The method of increasing signal bandwidth B is more effective than increasing SNR. So spread spectrum is a good method to increase the channel capacity. On the other hand, we can find from Eq.(3.1) that with a lower SNR we can achieve the same channel capacity with a higher signal bandwidth B. So signal can be transmitted in the case of lower SNR by using spread spectrum technology. Transmitting spread spectrum signal at low SNR can increase the

elusive of useful signal and decrease the possibility of being intercepted.

Here are some characteristics of spread spectrum [5]:

(1) High resistance ability to interferences.

The transmitted signal is spread to a wide frequency band by using spread spectrum technologies at the transmitter, and the received signal is restored to its original signal bandwidth by using correlative reception at the receiver. The EMI signals are uncorrelated to the spread signal, which are spread to a wide frequency band at the receiver. The power of EMI signals that can disturb the transmitted signal reduces greatly and the signal to interference ratio (SIR) at receiver increases correspondingly.

(2) High resistance ability to eavesdropping.

The spreading sequences with long duty and high complexity are unknown by anyone. So they are not easily to be intercepted and deciphered. Moreover, the power spectral density (PSD) of a spread spectrum signal is very low, which can be even lower than the PSD of noise. In such a case, it is difficult to detect the spread spectrum signal among the noise.

(3) High resistance ability to fading.

Frequency selective fading can only affect a small part of the bandwidth of the transmitted signal because of the wide bandwidth of spread spectrum.

(4) Capability of multiple accesses.

If multiple users use different spreading sequences, they can transmit information at the same time and frequency. There is little impact on each user.

3.1.2 Spreading gain

The anti-interference ability of a spread spectrum communication system is stronger than for a conventional communication system. We usually introduce the concept of spreading gain [6] to measure the anti-jamming ability of a spread spectrum communication system. In a spread spectrum system, the spreading gain G is defined as the ratio of de-spread spectrum output SNR of the receiver and the input SNR of the receiver.

$$G = \frac{S_0 / N_0}{S_i / N_i} \tag{3.2}$$

where S_0 / N_0 is the de-spread spectrum output SNR of receiver and S_i / N_i is the input SNR of receiver.

In a direct sequence spread spectrum system, the spreading gain is equal to the ratio of the pseudo-random sequence spread spectrum signal bandwidth (i.e. sequence spreading code rate R_c) to the information data signal bandwidth (i.e. the information data rate R_b).

$$G = \frac{R_c}{R_b} \tag{3.3}$$

The bigger spreading gain of the spread spectrum communication system is, the greater immunity to noise interference the system has.

3.2 Spread spectrum types

In this section, we introduce the spread spectrum types. The spread spectrum technologies have already been developing for nearly 70 years [5], and the main spread spectrum technologies are introduced as follows. They are direct-sequence spread spectrum and frequency-hopping spread spectrum respectively.

3.2.1 Direct-sequence spread spectrum (DSSS)

Direct-sequence spread spectrum [8] is the spread spectrum technique that is widely used. A DSSS communication system spreads the transmitted signal to a wide frequency band by a pseudonoise (PN) [9] code. The spread signal takes up more bandwidth than the original signal. At the receiver, the signal is restored to the original signal using the same PN code as at the transmitter.

Fig. 3.1 shows the working principle of DSSS. The rate of the PN sequence is much higher than the rate of the source data. So we apply repetition encoder to make their rates be the same. The PN sequence which is generated by the PN generator modulates the source data, then the signal bandwidth has been spread. The algorithm of source data and PN sequence is mode-2 addition. The spreading signal is transmitted over the channel after modulation. At the receiver, the same PN sequence is used as transmitter to demodulate the demodulated signal. And the transmitted data is restored after repetition decoder.

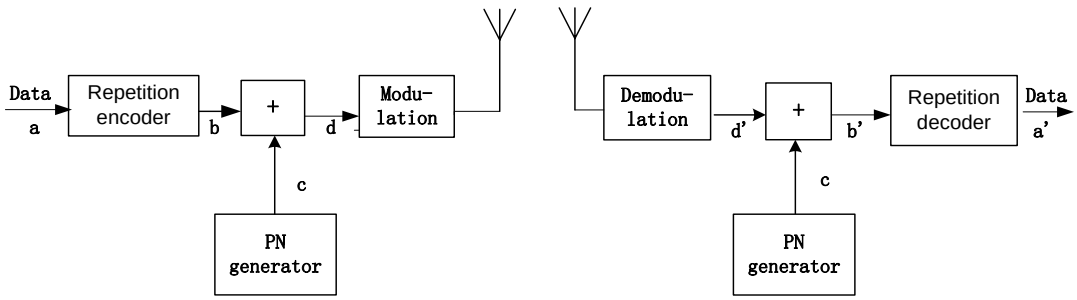

Fig. 3.1 working principle of DSSS

Fig. 3.2 indicates the specific transmission process diagram of DSSS. In this example, the rate of the PN sequence (c) is 10 times higher than the rate of the source data (a). So the bandwidth of the PN sequence (c) is 10 times wider than the bandwidth of the source data (a). The source data (a) becomes the repeated data (b) after repetition encoder. Then the rates of repeated data (b) and PN sequence (c) are the same. We can get the spreading data (d) after mode-2 addition of repeated data (b) and PN sequence (c). At the receiver, we use the same PN sequence (c) as at the transmitter to demodulate the received demodulated signal (d'). The source data (a') is recovered after repetition decoder, which is the same as the source data (a).

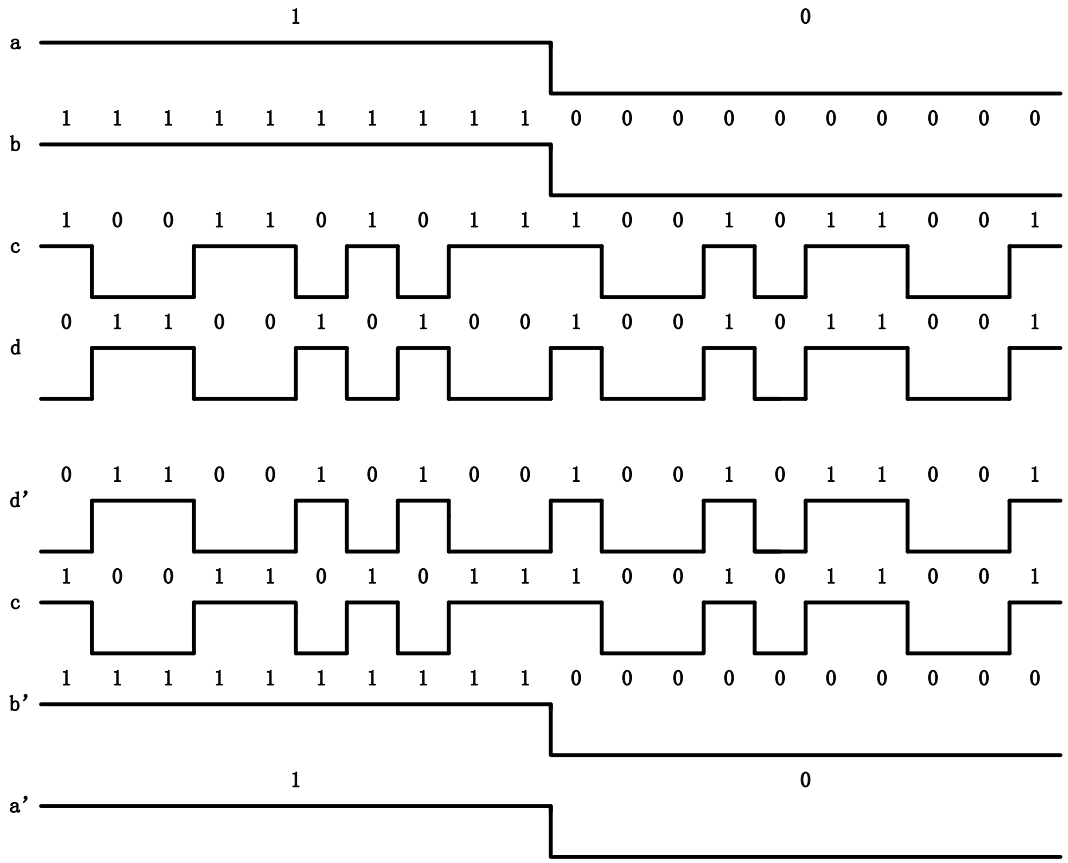

Fig. 3.2 transmission process diagram of DSSS signal

The process of DSSS can also be expressed by mathematical formulas. The source sequence $a(t)$ with data rate R_a and date period T_a can be expressed as eq.(3.4), where $T_a = 1/R_a$.

$$a(t) = \sum_{n=0}^{\infty} a_n w_a (t - nT_a) \tag{3.4}$$

where a_n is source data and w_a is the source window function, which can be expressed as:

$$a_n = \begin{cases} +1 & with\ probability\ P \\ -1 & with\ probability\ 1-P \end{cases}$$

and $w_a(t) = \begin{cases} 1 & 0 \le t \le T_a \\ 0 & others \end{cases}$

The PN sequence $c(t)$ can be expressed as eq. (3.5), with data rate R_c and data period T_c, where $T_c = 1/R_c$.

$$c(t) = \sum_{n=0}^{\infty} c_n w_c(t - nT_c) \tag{3.5}$$

In eq.(3.5), c_n is PN data and w_c is the pseudonoise window function, which can be expressed as:

$$c_n = \begin{cases} +1 & with\ probability\ P \\ -1 & with\ probability\ 1-P \end{cases}$$

and $w_c(t) = \begin{cases} 1 & 0 \le t \le T_c \\ 0 & others \end{cases}$

The essence of DSSS is mode-2 addition of source sequence $a(t)$ and PN sequence $c(t)$, which also can be seen as multiplication of them. The rate of PN sequence R_c is much higher than the rate of source sequence R_a, and the value of R_c/R_a is an integer. So the rate of the spreading sequence is R_c, the same as the PN sequence rate. The expression of the spreading sequence is:

$$d(t) = a(t)c(t) = \sum_{n=0}^{\infty} d_n w_c(t - nT_c) \tag{3.6}$$

where $d_n = \begin{cases} +1 & c_n = a_n \\ -1 & c_n \neq a_n \end{cases} \quad (n-1)T_c \leq t \leq nT_c$

DSSS spread the transmitted signal to a very wide frequency band, and makes the PSD lower. The lower PSD signal is transmitted over the channel among the noise, and becomes hard to be detected.

The demodulated signal at receiver is $d'(t) = a(t)c(t) + n(t) + J(t)$ (3.7)

where $n(t)$ is noise and $J(t)$ is the interference signal.

Then the de-spread process is:

$$\begin{aligned} d'(t)c(t) &= (a(t)c(t) + n(t) + J(t))c(t) \\ &= a(t)c^2(t) + (n(t) + J(t))c(t) \\ &= a(t) + n(t)c(t) + J(t)c(t) \end{aligned} \quad (3.8)$$

Because the values of the spread sequence $c(t)$ are +1 and -1, $c^2(t) = 1$. It is uncorrelated between spread sequence $c(t)$, noise $n(t)$ and interference signal $J(t)$. The signal $a(t)$ is a narrow band signal, and the signals $n(t)c(t)$ and $J(t)c(t)$ are wide band signals. Then the transmitted data are recovered even when noise and interference signal exist. The DSSS communication system has good characteristics of high resistance ability to EMI and noise.

3.2.2 Frequency-hopping spread spectrum (FHSS)

The fixed carrier frequency communication system can be easily detected by others, while frequency-hopping spread spectrum [10] communication system is hardly possible to be discovered, since the operating frequency of a FHSS communication system is changing all the time. When others find the transmission frequency, the working frequency has already changed to another frequency. Thus it is hard to disturb the FHSS communication system unless the frequency changing rule is leaked. So this communication system has high resistance ability to EMI and eavesdropping.

In FHSS technology the carrier frequency of the communication system is changing rapidly and randomly with a PN sequence. The PN sequence is only known by the transmitter and the receiver. The PN sequence will not be transmitted from transmitter to receiver directly, but only used to select the working frequency with the PN sequence known beforehand by the transmitter and the receiver.

At the receiver, the frequency of the received signal is recovered using the same PN sequence as at the transmitter. The interference signal doesn't know the frequency changing rule, thus it has typically no correlation with the frequency-hopping signal. So it can't interference this frequency-hopping system too much, and it has high resistance ability to interferences. Fig. 3.3 shows the working principle of FHSS.

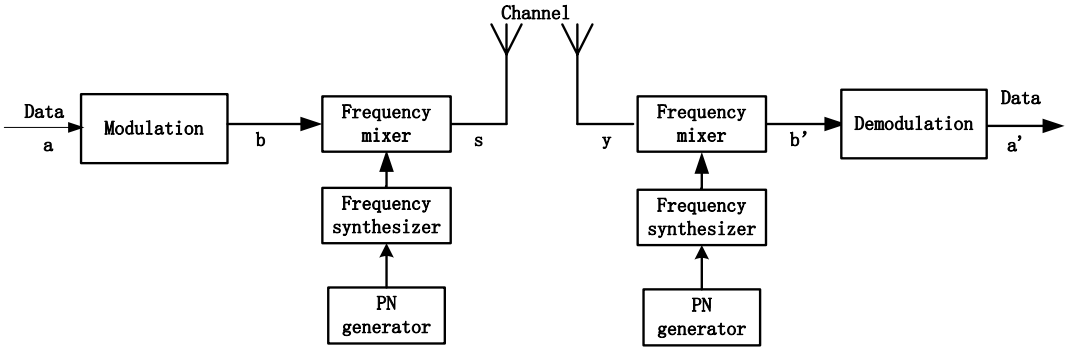

Fig. 3.3 working principle of FHSS

The process of FHSS can also be expressed by mathematical formulas. The transmitted signal after frequency-hopping $s(t)$ can be expressed as

$$s(t) = b(t)\cos[(\omega_0 + n\Delta\omega)t + \varphi_0] \tag{3.9}$$

where $b(t)$ is the transmitted signal after modulation;

$\cos[(\omega_0 + n\Delta\omega)t + \varphi_0]$ is frequency-hopping signal, which is the output signal of frequency synthesizer;

$n = 0,1,2,\cdots,N-1$;

$\Delta\omega$ is frequency separation of frequency synthesizer, $\Delta\omega = 2\pi / T$, and T is every frequency-hop period;

φ_0 is initial phase.

The receiver receives the signal $y(t)$ which can be expressed as follows:

$$y(t) = s(t) + n(t) + J(t) \tag{3.10}$$

where $s(t)$ is transmitted signal;

$n(t)$ is noise;

$J(t)$ is interference signal.

The received signal $y(t)$ multiplies the frequency-hopping signal with $\cos[(\omega_0 + n\Delta\omega)t + \varphi_0]$, then we can get the signal $b'(t)$ before demodulation.

$$\begin{aligned} b'(t) &= y(t)\cos[(\omega_0 + n\Delta\omega)t + \varphi_0] \\ &= [s(t) + n(t) + J(t)]\cos[(\omega_0 + n\Delta\omega)t + \varphi_0] \\ &= \frac{1}{2}b(t)[1 + \cos[2(\omega_0 + n\Delta\omega)t + 2\varphi_0]] + [n(t) + J(t)]\cos[(\omega_0 + n\Delta\omega)t + \varphi_0] \\ &= \frac{1}{2}b(t) + \frac{1}{2}b(t)\cos[2(\omega_0 + n\Delta\omega)t + 2\varphi_0] + [n(t) + J(t)]\cos[(\omega_0 + n\Delta\omega)t + \varphi_0] \end{aligned} \tag{3.11}$$

We can get useful component $b(t)$ after signal $b'(t)$ passing through a filter. Then we can get the transmitted data $a(t)$ after demodulation.

The bandwidth of the frequency-hopping signal is narrow in a signal frequency-hop period. But the frequency-hopping speed is very fast, and the signal is hopping in a wide frequency band to form a wide hopping bandwidth. So frequency-hopping realizes the spectrum spreading on a macro level because of the fast speed of frequency-hopping.

The period of the PN sequence is very large and its complexity is very high. So it is very difficult to detect the PN sequence changing rule by an intentional interferer. Thus, the FHSS communication system has good characteristics of high resistance ability to EMI and eavesdropping.

3.3 Channel Coding

In this section, we introduce the channel coding technologies. As we know, errors will appear during the transmission because of non-ideal channel and additive white Gaussian noise (AWGN). The system BER will decrease if channel coding techniques are used. The main idea of channel coding is to add redundancy to the transmitted signal. Because of redundancy, the receiver can detect some errors and correct them without retransmission while the number of errors is less than its impairment ability [6]. The channel coding techniques we introduce here are cyclic redundancy check, Reed–Solomon codes and interleaving.

3.3.1 Cyclic redundancy check (CRC)

Cyclic redundancy check is an error-detecting code, which can only detect whether any error happened during the transmission. I.e. CRC has no error correction ability, so it requires the transmitter to retransmit the message while errors are found.

Cyclic redundancy check was first proposed by W. Wesley Peterson in 1961 [11], and it is widely used in modern communication systems. At the transmitter, a short check value sequence is derived from calculation of a special length message and polynomial [11] division. Then the short check value sequence is attached to the end of the special length message, and transmitted them together with the message. At the receiver, another short check value is derived by repeating the calculation of the received message and the same polynomial division. If the short check value is '1', it means errors happened during the transmission and the transmitter is required to retransmit the message.

Now assume the input frame m length of CRC encoder is n, the degree of the polynomial division b is r, and generate k checksums in every frame. The processes of CRC encoders are as follows.

(1) Divide the input frame m into k parts to form sequence n_i, and the length n_i is n/k;

(2) Pad r bits zeros to the end of every part frame n_i to form a new sequence n_i';

(3) Calculate the check value a_i by the polynomial division b and n_i';

(4) Add every a_i to the end of every n_i to form the sequence n_i'';

(5) Join every n_i'' one by one to form the new transmit sequence m';

The processes of CRC decoders are as follows.

(1) Divide the received frame m'' into k parts to form sequence c_i, and the length c_i is $n/k + r$;

(2) Calculate the check value d_i by the same polynomial division b and c_i;

(3) The result we get is '0' means no error happened, otherwise, some errors happened during the transmission.

The CRC used on the SPCS is CRC (237, 225), and the generator polynomial $g(x)$ can be expressed as the following equation [12].

$$g(x) = x^{12} + x^{11} + x^3 + x^2 + x + 1 \tag{3.12}$$

3.3.2 Reed–Solomon (RS) codes

Reed–Solomon codes were invented by Irving S. Reed and Gustave Solomon in 1960 [13], which have very good error correction performance. RS codes can correct both random and burst errors.

Reed-Solomon codes can be seen as cyclic BCH codes. The encoding symbols are the coefficients of a polynomial derived by multiplying $p(x)$ with $g(x)$. The transmitted data can be seen as coefficients of the polynomial $p(x)$.

The generator polynomial $g(x)$ can be expressed as [22]:

$$g(x) = (x-\alpha)(x-\alpha^2).....(x-\alpha^{d-1}) \tag{3.13}$$

Reed–Solomon codes can be expressed as RS (n, k). The length of code is n, the input data dimension is k, and the minimum Hamming distance is $n-k+1$. If Reed–Solomon codes don't know positions of errors in advance, it can correct up to $(n-k)/2$ errors. Otherwise,

it can judge up to $n-k$ bits data. [14]

The Reed-Solomon codes used on the SPCS is RS (31, 15) correction coding. The generated polynomial $g(x)$ can be expressed as follows [22].

$$g(x)=\prod_{i=1}^{16}(x-\alpha^{i})=x^{16}+\alpha^{23}x^{15}+\alpha^{13}x^{14}+x^{13}+\alpha^{8}x^{12}+\alpha^{3}x^{11}+\alpha x^{10}+\alpha^{21}x^{9} \\ +\alpha^{25}x^{8}+\alpha^{7}x^{7}+\alpha^{4}x^{6}+\alpha^{2}x^{5}+\alpha^{14}x^{4}+\alpha^{23}x^{3}+\alpha^{22}x^{2}+\alpha^{18}x+\alpha^{12} \quad (3.14)$$

The minimum Hamming distance of RS (31, 15) codes is $d=n-k+1=17$, and its error correction ability is $(d-1)/2=8$. So if the data amount is less than 16 bits, it can't be judged at the receiver, RS (31, 15) codes can decide all those data correctly. Even if 8 bits data are misjudged, RS (31, 15) codes can correct all the errors.

3.3.3 Interleaving and deinterleaving

Interleaving and deinterleaving [15] are commonly used in communication systems, which can improve the error correction ability of Reed–Solomon codes. Data always transmit over the channel with a burst error. As we mentioned before, if the number of errors exceeds the correcting ability of Reed–Solomon codes, Reed–Solomon codes will lose any error correcting capability. Interleaving shuffles the transmitted data, which also disperses the burst errors and creates a balanced error distribution [15]. Therefore, interleaving and Reed–Solomon codes being used together is a good cooperation to decrease the BER.

Fig. 3.4 shows an example of transmitting over a burst error channel with interleaving and deinterleaing. We can see from fig. 3.4 that interleaving makes the burst errors to be uniformly distributed in the messages. Then the number of errors in each frame does not exceed the error correcting ability of Reed–Solomon codes. Therefore, all the errors can be corrected at the receiver.

	Frame 1:			Frame 2:			Frame 3:			Frame 4:		
Transmitted messages:	1	2	3	4	5	6	7	8	9	10	11	12
Interleaved messages:	1	4	7	10	2	5	8	11	3	6	9	12
Messages after burst errors:	1	4	7				8	11	3	6	9	12
Received deinterleaved messages:	1		3	4		6	7	8	9		11	12

Fig. 3.4 transmission with interleaving and deinterleaing

Fig. 3.5 shows an example of transmitting over a burst error channel without interleaving and deinterleaing. We can see from fig. 3.5 that burst errors happened among the received messages. The errors may appear in one frame, the number of which may exceed the error correcting ability of Reed–Solomon codes. So Reed–Solomon codes may fail to correct the errors.

	Frame 1:			Frame 2:			Frame 3:			Frame 4:		
Transmitted messages:	1	2	3	4	5	6	7	8	9	10	11	12
Messages after burst errors:	1	2	3				7	8	9	10	11	12
Received messages:	1	2	3				7	8	9	10	11	12

Fig. 3.5 transmission without interleaving and deinterleaing

3.4 BPSK modulation

The modulation mode of the SPCS is Binary Phase-shift keying (BPSK). BPSK is the simplest mode of Phase-shift keying, which transmit s data using two opposite phases, 0^o and 180^o. BPSK has the highest ability to resist noise and interferences among all of Phase-shift keying.

The equations of BPSK signals are as follows [16]:

$$s_0(t) = \sqrt{\frac{2E_s}{T}}\cos(\omega_c t + \pi) = -\sqrt{\frac{2E_s}{T}}\cos(\omega_c t) \qquad \text{for data '0'} \qquad (3.15)$$

$$s_1(t) = \sqrt{\frac{2E_s}{T}} \cos(\omega_c t) \qquad \text{for data '1'} \qquad (3.16)$$

where ω_c is carrier frequency, E_s is symbol energy and T is symbol period.

The upper equations can also be merged to be the following equation:

$$s_n(t) = \sqrt{\frac{2E_s}{T}} \cos(\omega_c t + \pi(1-n)), n = 0,1 \qquad (3.17)$$

where n is the transmitting data '0' and '1'.

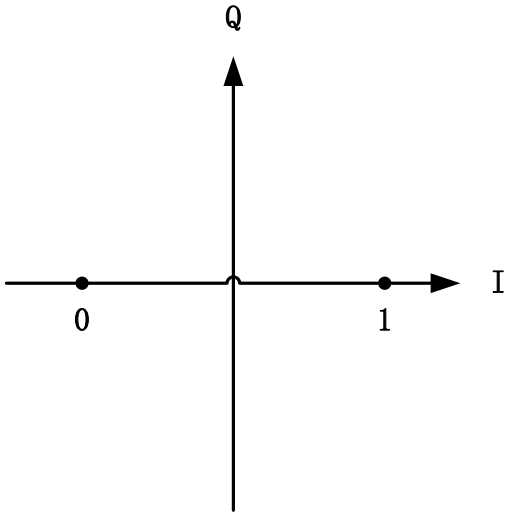

Fig. 3.6 Constellation diagram of BPSK

Fig. 3.6 shows the constellation diagram of BPSK. The BER [17] of BPSK in AWGN channel is:

$$P_{BPSK} = \frac{1}{2} erfc\left(\sqrt{\gamma}\right) \qquad (3.18)$$

where $erfc(x) = \frac{2}{\sqrt{\pi}} \int_x^\infty \exp\left(-y^2\right) dy$ and $\gamma = \frac{A^2}{2\sigma^2}$ is signal to noise ratio.

4 Electromagnetic Interference signals

The basic principle of EMI signals in communication is to destroy the capacity of receiving the correct information. The principal types of jamming signals on communication systems are tone jamming and noise jamming [18][19]. The main types of noise jamming include noise amplitude modulation jamming, random binary code modulation jamming and PN code MSK modulation jamming. Tone jamming includes both single tone jamming and multiple tones jamming. These jamming signals are blanket jamming [6]. Blanket jamming is used to make the opponents' received useful signals to be obscured or completely covered. So opponents' communication is interrupted. The main EMI damage to SPCS we designed is the blanket jamming, so we will discuss blanket EMI signals in this thesis.

In this chapter, we will introduce these EMI signals [20]. These EMI signals will be added into the DSSS and FHSS system we built to estimate the resisting EMI ability of these communication systems.

4.1 Noise amplitude modulation jamming signal

Noise amplitude modulation jamming signal is a common jamming signal in communication. The equation of noise amplitude modulation jamming signal can be expressed as below.

$$J(t) = An(t)\cos\left[\omega_c t + \phi_0\right] \tag{4.1}$$

where ω_c is carrier frequency, ϕ_0 is carrier initial phase, A is carrier amplitude, and $n(t)$ is Gaussian noise with mean 0 and variance σ_n^2.

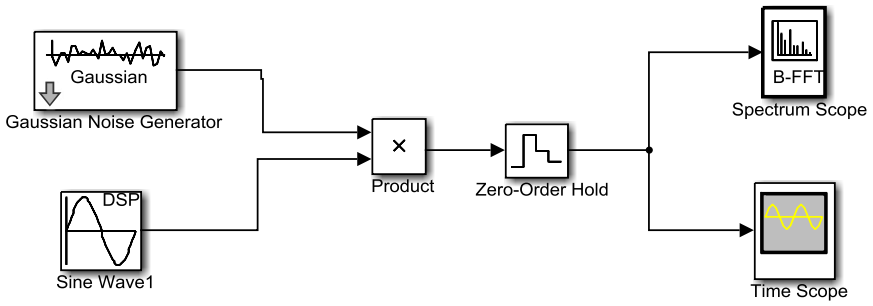

Fig. 4.1 noise amplitude modulation jamming signal simulation model

The above figure shows the noise amplitude modulation jamming signal simulation model in

Simulink. The parameters of the model are set as follows: the sample time of the Gaussian noise generator is 1e-5s, the carrier frequency of the sine wave is 1 MHz, and the sample time of the zero-order hold is 1e-7s. The simulation results are shown in the following figures.

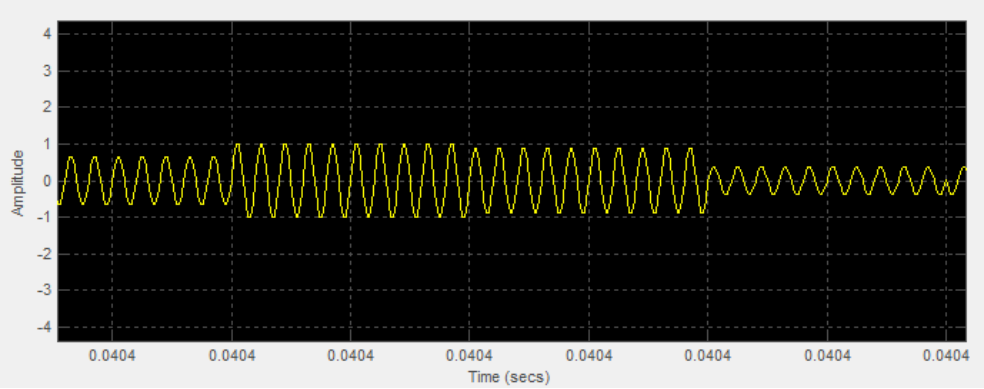

Fig. 4.2 time domain waveform of noise amplitude modulation jamming signal

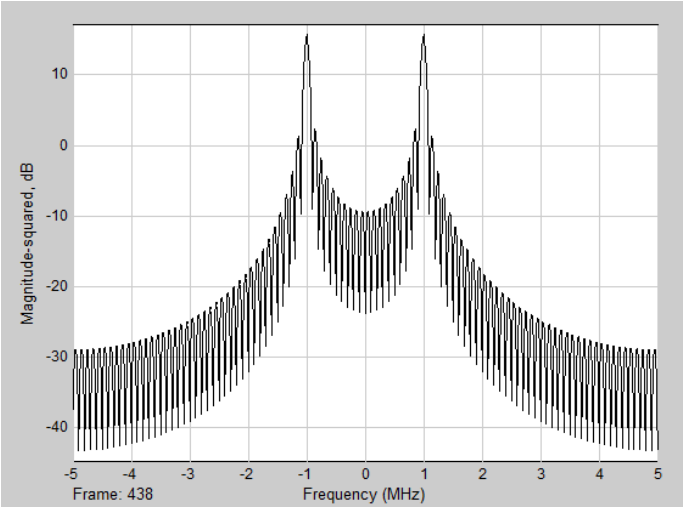

Fig. 4.3 frequency spectrogram of noise amplitude modulation jamming signal

4.2 Random binary code modulation jamming signal

The equation of noise amplitude modulation jamming signal can be expressed as below.

$$J(t) = A\sum_{n=0}^{+\infty} J_n g(t - nT_j)\cos(2\pi f_c t + \phi) \tag{4.2}$$

where A is jamming signal amplitude, $J_n = \pm 1 \ \ (0 \le n < \infty)$ is a random sequence, $g(t)$

is a rectangular pulse with width T_j, ϕ is carrier initial phase, and f_c is carrier frequency.

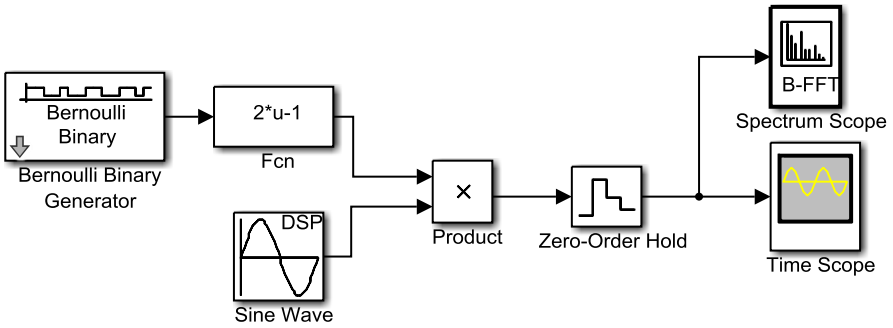

Fig. 4.4 random binary code modulation jamming signal simulation model

The above figure shows frequency spectrogram of the simulation model in Simulink. The parameters of the model are set as follows: the sample time of the Bernoulli binary generator is 1e-5s, the carrier frequency of the sine wave is 1 MHz, and the sample time of the zero-order hold is 1e-7s. The simulation results are shown in the following figures.

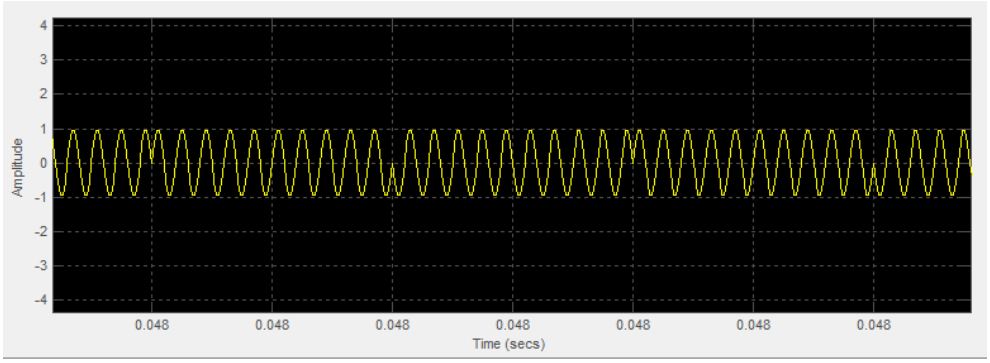

Fig. 4.5 time domain waveform of random binary code modulation jamming signal

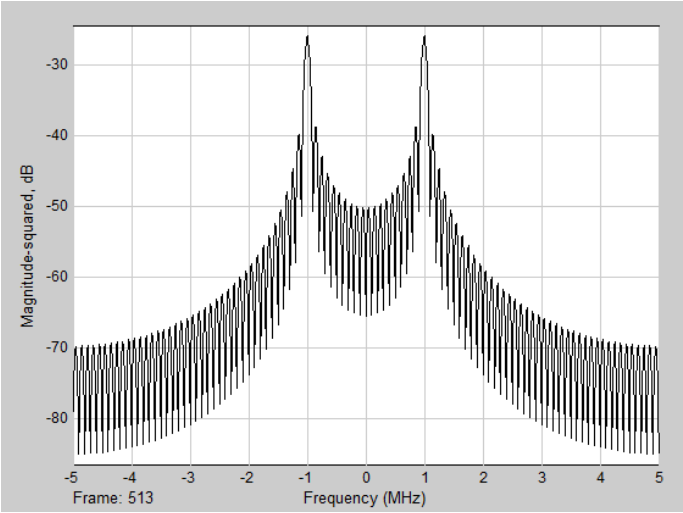

Fig. 4.6 frequency spectrogram of random binary code modulation jamming signal

4.3 PN code MSK modulation jamming signal

An MSK modulator is used to modulate the PN sequences, and then the modulated signal is moved to interference frequency. When we use the same PN sequences as in the DSSS codes, the PN code MSK modulation jamming signal can maximize access to the receiver. And it can produce good interference effect.

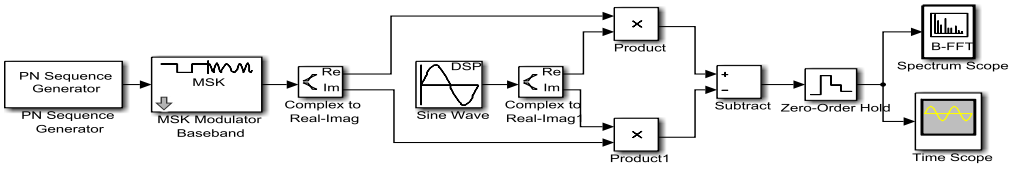

Fig. 4.7 PN code MSK modulation jamming signal simulation model

The above figure shows the PN code MSK modulation jamming signal simulation model in Simulink. The parameters of the model are set as follows: the sample time of PN sequence generator is 1e-5s, the carrier frequency of the sine wave is 1 MHz, and the sample time of the zero-order hold is 1e-7s. The simulation results are shown in the following figures.

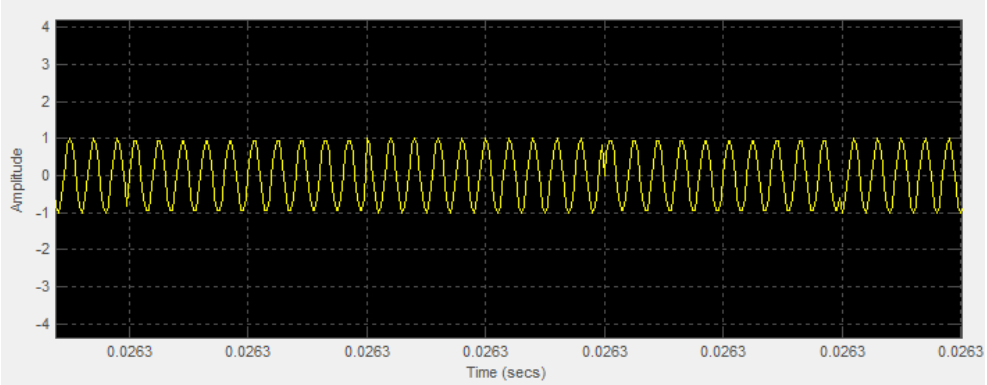

Fig. 4.8 time domain waveform of PN code MSK modulation jamming signal

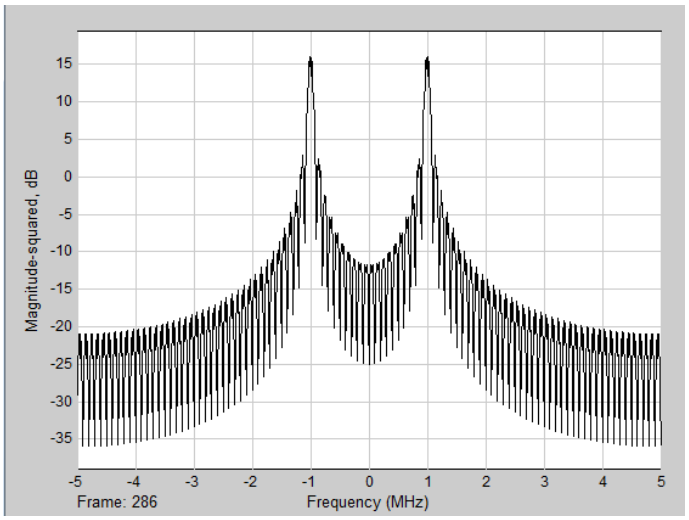

Fig. 4.9 frequency spectrogram of PN code MSK modulation jamming signal

4.4 Tone jamming signal

Tone jamming can be divided into single tone jamming and multiple tones jamming. Single tone jamming signal can only interfere at one frequency point. Multiple tones jamming signal can disturb at parts of frequency points in the frequency-hopping communication system. The schematic diagram can be seen as below.

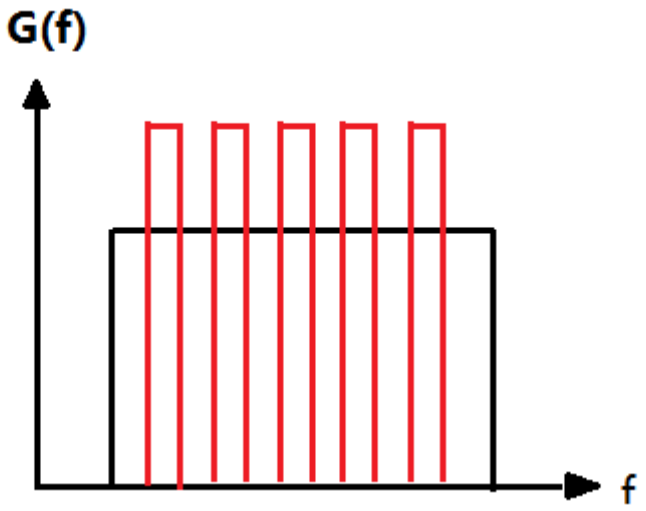

Fig. 4.10 schematic diagram of multiple tones jamming signal

The equations of a single tone and multiple tones jamming signal can be expressed as Eq.(4.3) and Eq.(4.4), respectively.

$$J(t) = A\cos\left[\omega_c t + \phi_0\right] \tag{4.3}$$

$$J(t) = A\cos\left[\omega_{c_1} t + \varphi_0\right] + A\cos\left[\omega_{c_2} t + \varphi_0\right] + \ldots A\cos\left[\omega_{c_n} t + \varphi_0\right] \tag{4.4}$$

where ω_c is carrier frequency, ϕ_0 is carrier initial phase and A is carrier amplitude.

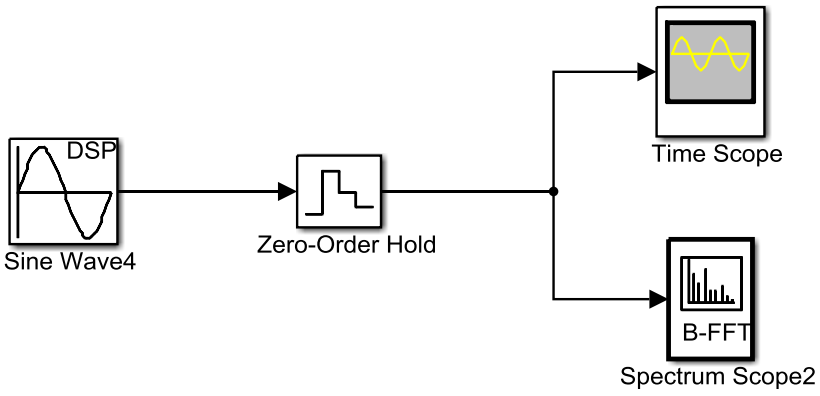

Fig. 4.11 single tone jamming signal simulation model

Fig. 4.11 shows the single tone jamming signal simulation model in Simulink. The parameters of the model are set as follows: the carrier frequency of the sine wave is 1 MHz, and the sample time of the zero-order hold is 1e-7s. The simulation results are shown in the following

figures.

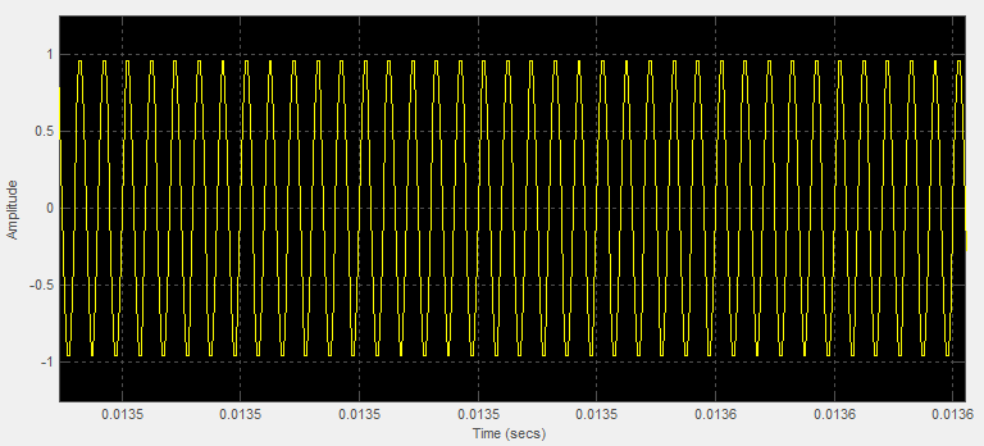

Fig. 4.12 time domain waveform of single tone jamming signal

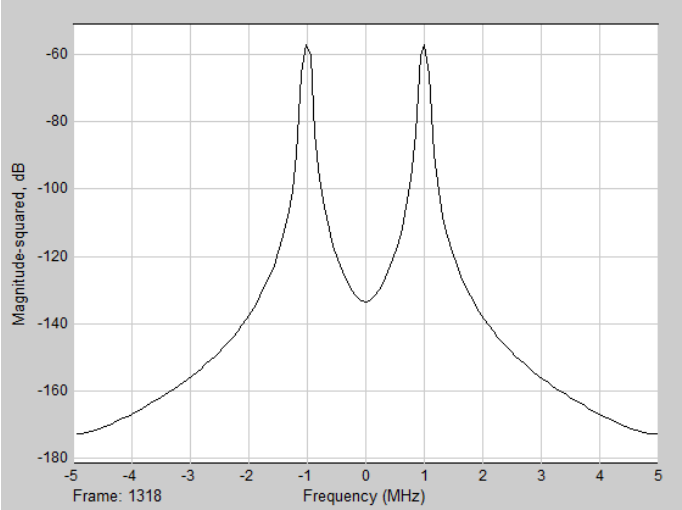

Fig. 4.13 frequency spectrogram of single tone jamming signal

Multiple tones jamming signal is similar to partial-band noise jamming, which is useful to deal with the frequency-hopping communication system.

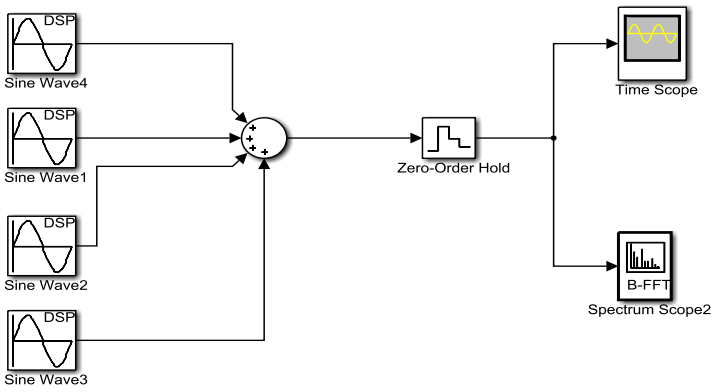

Fig. 4.14 multiple tones jamming signal simulation model

Fig. 4.14 shows the multiple tones jamming signal simulation model in Simulink. The parameters of the model are set as follows: the carrier frequencies of the sine wave are 1 MHz, 2 MHz, 3 MHz and 4 MHz, and the sample time of the zero-order hold is 1e-7s. The simulation results are shown in the following figures.

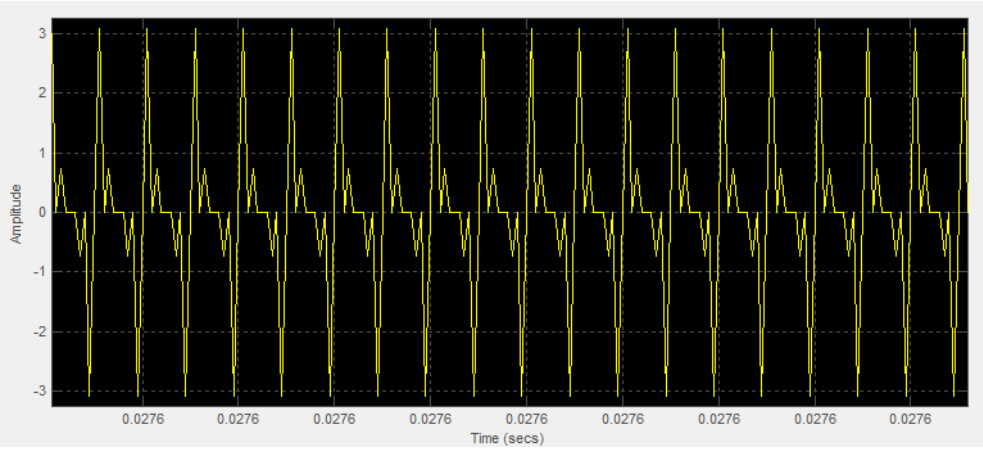

Fig. 4.15 time domain waveform of multiple tones jamming signal

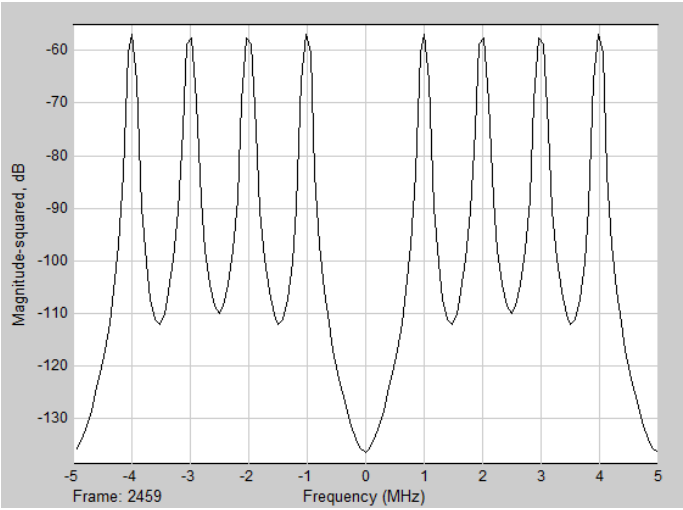

Fig. 4.16 frequency spectrogram of multiple tones jamming signal

5 Modeling and simulation results

The software ADS and Matlab/Simulink were used to build both the block-level and the system-level SPCS. We can get the BER curves to estimate the built system performance. Different EMI signals are introduced into the designed data link SPCS. The techniques of DSSS and FHSS are applied for improving the communication performance of the data link system we designed.

5.1 ADS simulation

In this section, we use the software ADS to build block-level modules, and then to build the system-level simulation model using the block-level modules.

5.1.1 Principle and packaging of different modules

(1) direct-sequence spread spectrum module

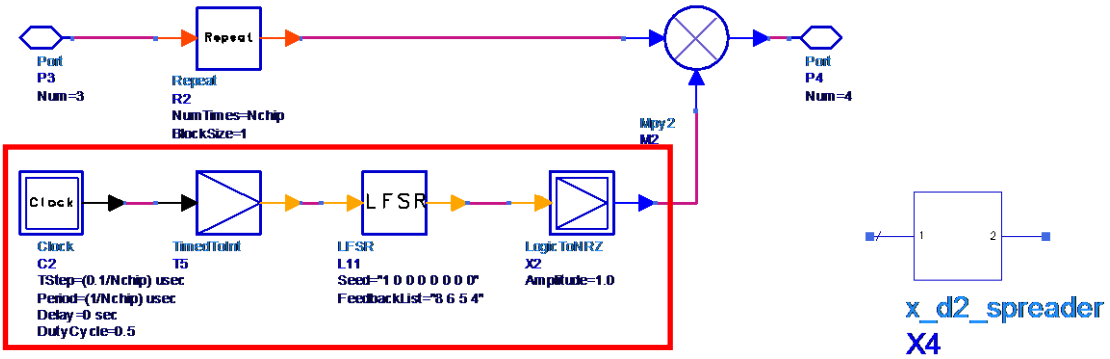

(a) (b)

Fig. 5.1 (a) principle of spread spectrum module (b) packaging of spread spectrum module

The devices in red block are used to generate a pseudorandom sequence, and its data rate is Nchip times than the input data. Then Nchip times spread spectrum can be achieved by multiplying two channel sequences.

(2) de-direct-sequence spread spectrum module

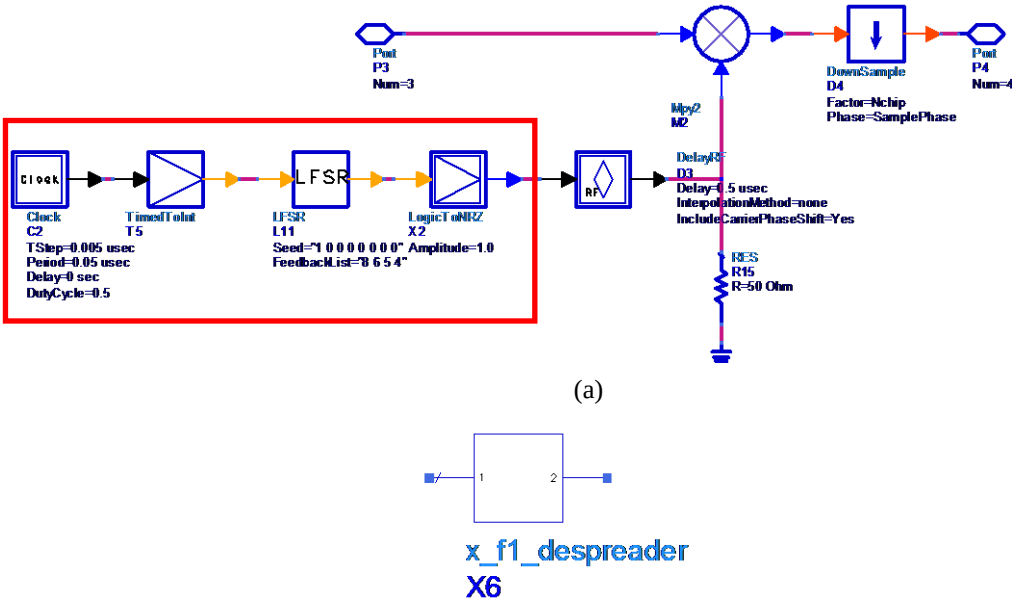

(a)

(b)

Fig. 5.2 (a) principle of de-spread spectrum module (b) packaging of de-spread spectrum module

The devices in red block are used to generate the same pseudorandom sequence as spread spectrum at the transmitter. To process multiplied signal through the device ‘downsample’, the input signal is de-spread. The delay of the system should be considered to make sure synchronization between the input signal and pseudorandom sequence signal.

(3) frequency-hopping module

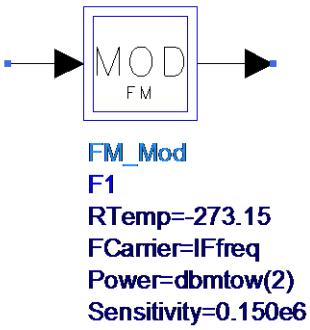

Fig. 5.3 principle of frequency-hopping module

It is impossible to build a module to realize the frequency-hopping function, so we can only use the frequency-shift keying (FSK) modulation module to replace the frequency-hopping module. It is used with the Bluetooth simulation example [21] in ADS as a reference. The carrier frequency variation of FSK modulation is similar to the frequency-hopping theory. The output formula of FSK modulation module is:

$$V_2(t) = A\cos\left(2\pi f_c t + 2\pi s\int_0^t V_1(\alpha)d\alpha\right) \tag{5.1}$$

where s is sensitivity and f_c is carrier frequency.

(4) de-frequency-hopping module

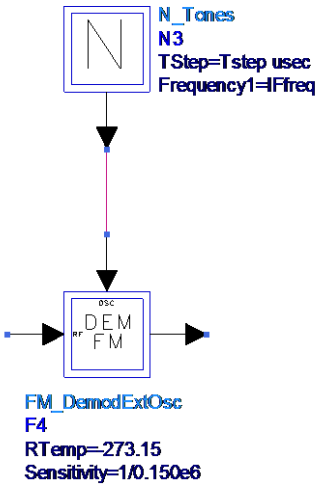

Fig. 5.4 principle of de-frequency-hopping module

We use the FSK demodulation module to achieve de-frequency-hopping, and we set the parameters of the FSK demodulation module to be the same as in the FSK modulation module, so that the signal received can be de- frequency-hopping.

(5) transmitter non-linear module

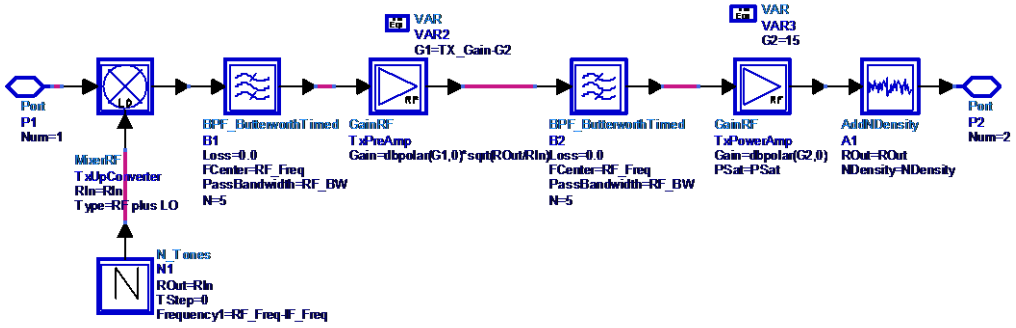

（a）

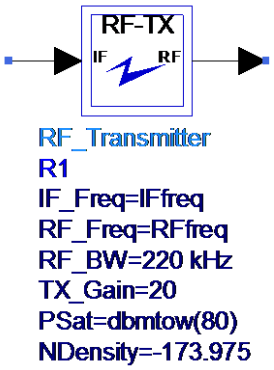

（b）

Fig. 5.5 (a) principle of transmitter module (b) packaging of transmitter module

The intermediate frequency signal becomes a radio frequency signal after passing through the mixer. The buterworth filter filters out the harmonics generated by the mixer, and amplifying the signal by the non-linear gain amplifier module. Then the secondary filtering and amplification, and the noise module (AddNDensity) increase Gaussian noise of the transmitter module. This transmitter module is the module which had been built in ADS, we only need to set the parameters.

The transmitter nonlinear characteristics can be simulated in ADS rather than Simulink. The nonlinear distortion character of the package module depends on the parameter Psat (saturated output power). When output power of this module exceeds the set value Psat, the transmitter output power no longer increases as the input power increases, but remains as a fixed value. This reflects the transmitter nonlinearity characteristics.

The non-linear gain of the transmitter module is 20dB, and the saturated output power Psat we set is 80dBm.

(6) receiver RF front end module

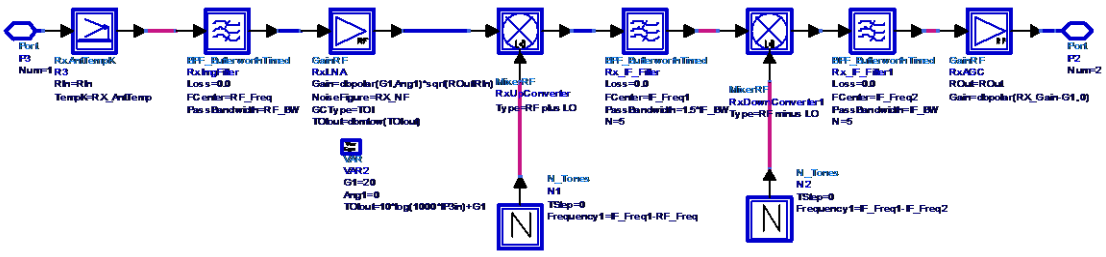

（a）

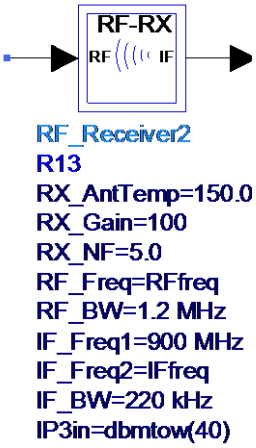

（b）

Fig. 5.6 (a) principle of receiver module (b) packaging of receiver module

Receiver RF front-end module is constructed as follows. Firstly we introduce Gaussian white noise caused by the receiving antenna temperature by the antenna noise module (RxAntTempK), then the signal is filtered through the band-pass Butterworth filter module (BPF_ButerworthTimed) and amplified by the low noise amplifier module. Finally the signal is amplified secondly by the automatic gain amplifier module (GainRF) after two times of down frequency conversions and harmonic filtering. This transmitter module is also the module which had been built in ADS, we only need to set the parameters.

Receiver RF front-end module gain is 100 dB and noise figure is 5 dB.

(7) antenna module

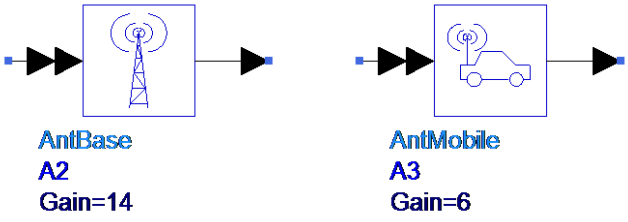

（a） （b）

Fig. 5.7 (a) transmitter antenna module (b) receiver antenna module

We select a base station and a mobile antenna at transmitter and receiver separately, and the antenna gain is 14 dB and 6dB respectively.

(8) channel module

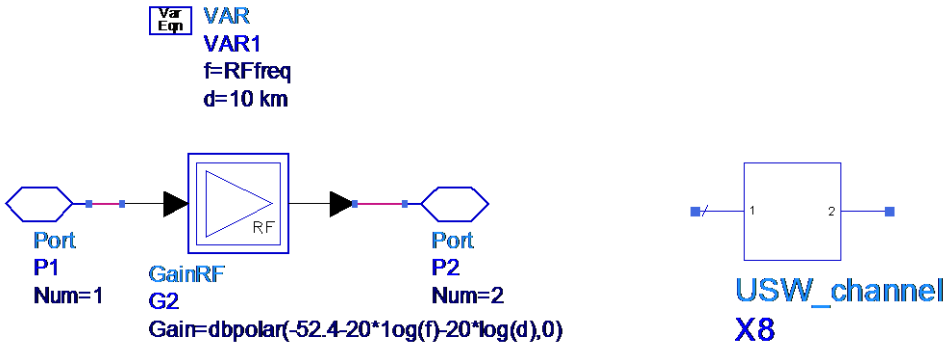

（a） （b）

Fig. 5.8 (a) principle of channel module (b) packaging of channel module

We consider the free space loss in the channel. Free space loss can be expressed as the following equation.

$$L_p = 32.4 + 20\log f + 20\log d \tag{5.2}$$

where L_p is free space loss, f is frequency and d is transmission distance.

(9) sampling module

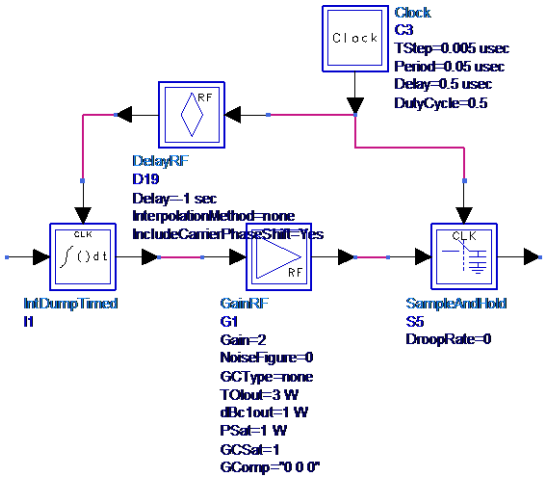

Fig. 5.9 principle of sampling module

Sampling module is used to sample the analog signal to be digital signal at receiver. Then the sampled digital data is transmitted to the de-spread spectrum module.

5.1.2 Direct-sequence spread spectrum

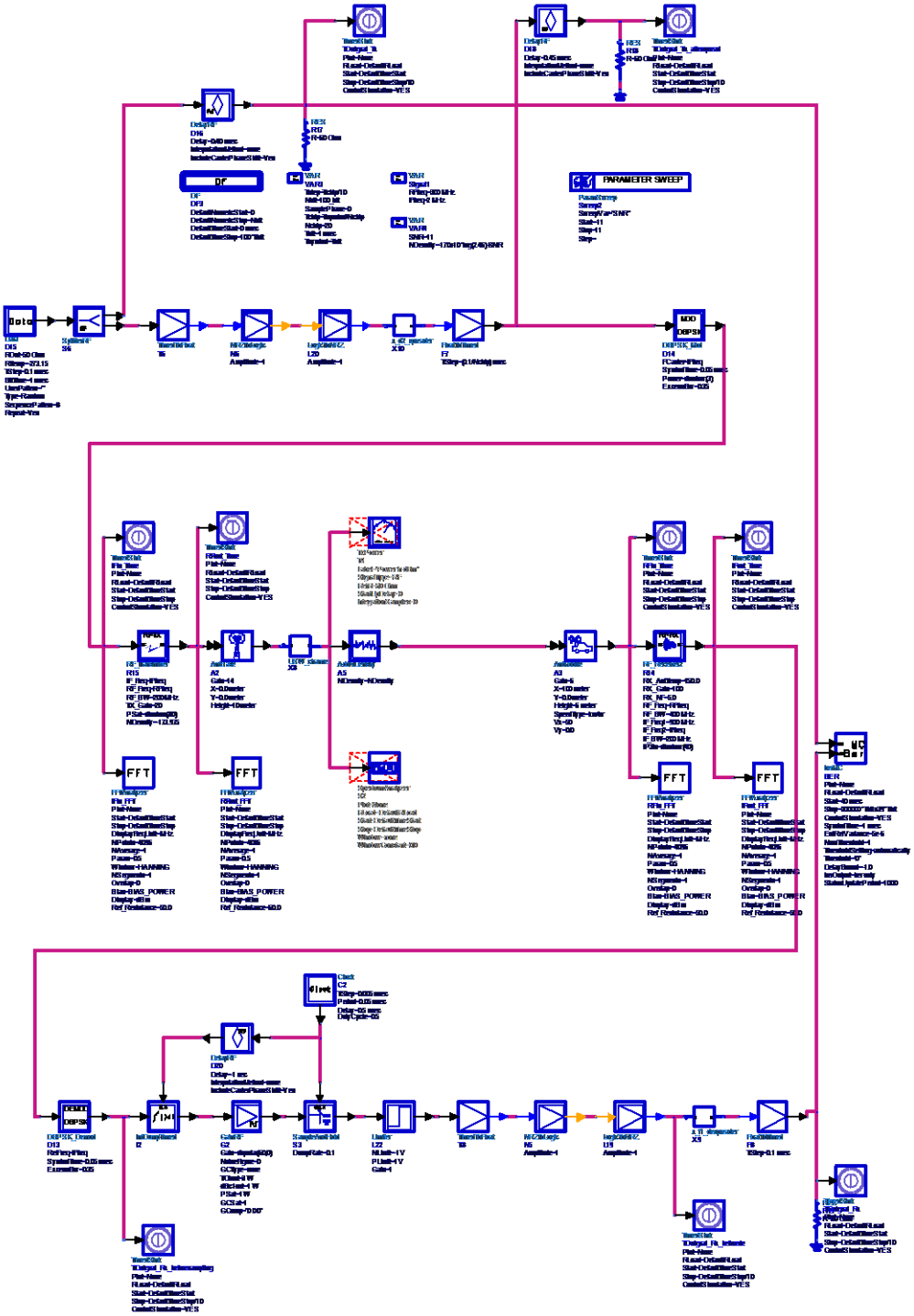

Fig. 5.10 BPSK modulation DSSS simulation model

The work principle of BPSK modulation DSSS simulation model is showed in Fig. 5.10,

which is composed by the modules we built in section 5.1.1. This simulation model realizes 10 times DSSS. The modulation we used in this model is BPSK. The transmitter modulates the transmitted signal to ultra-short wave spectrum 300 MHz. Then we can get the following figures after simulation.

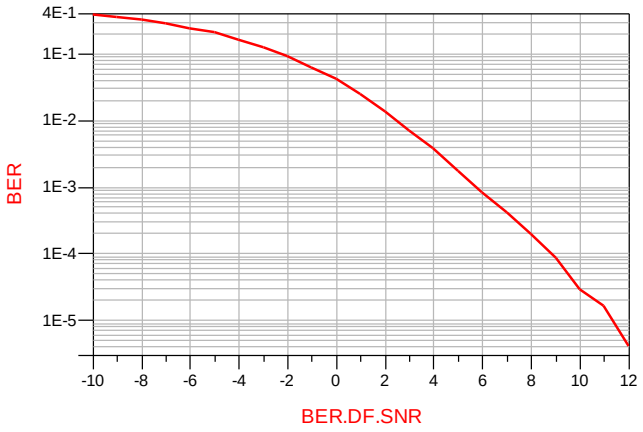

(a) BER of BPSK modulation DSSS

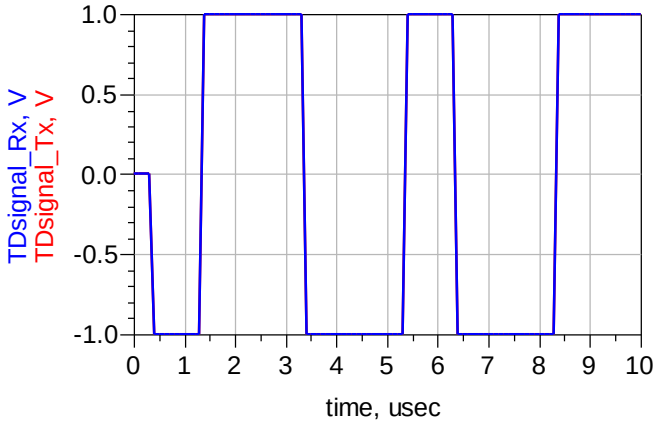

(b) time domain waveform of input and output

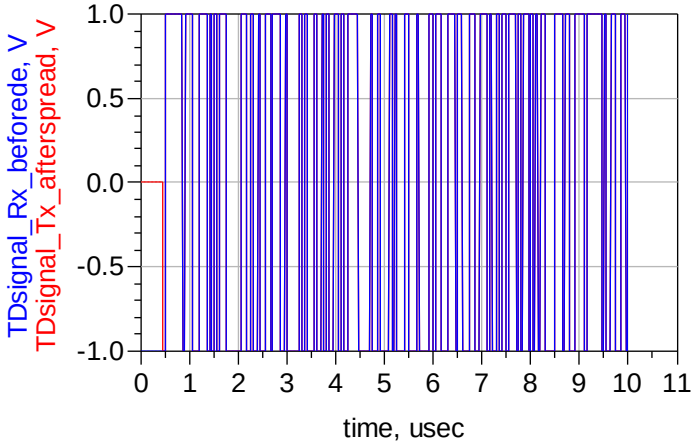

(c) time domain waveform of spread and de-spread signal

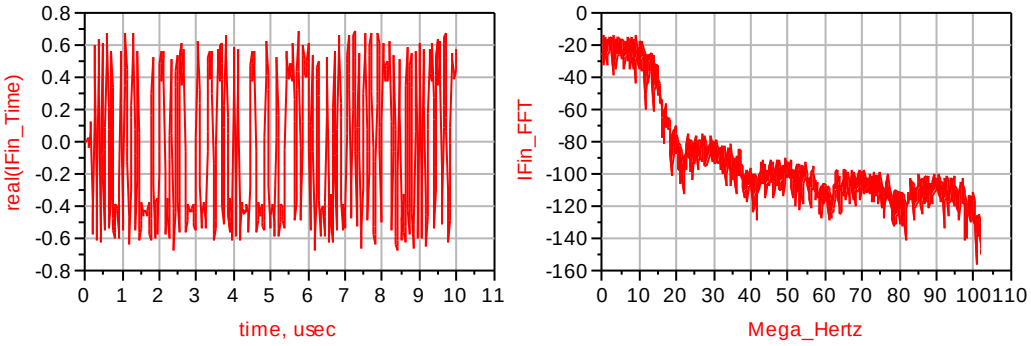

(d) time domain waveform of BPSK modulation (e) frequency spectrogram of BPSK modulation

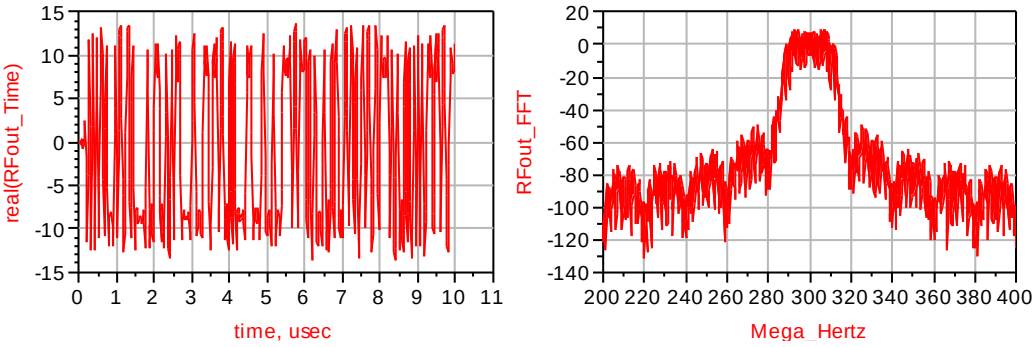

(f) time domain waveform of transmitter (g) frequency spectrogram of transmitter

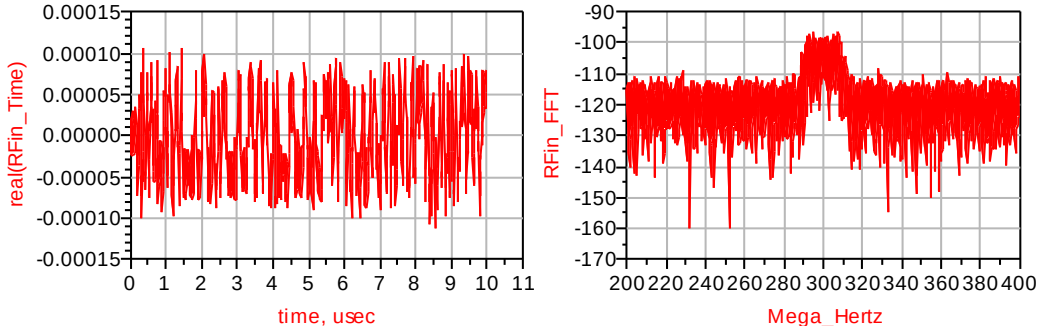

(h) time domain waveform of receiver input (i) frequency spectrogram of receiver input

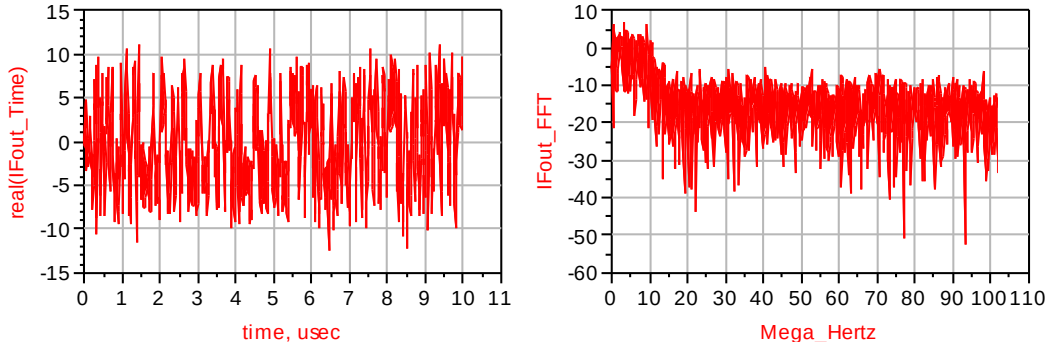

(j) time domain waveform of receiver output (k) frequency spectrogram of receiver output

Fig. 5.11 simulation results of BPSK modulation DSSS

We can see from fig. 5.11 (a) that the BER decreases with the increase of SNR, and this system is good at resisting the AWGN. Comparing fig. 5.11 (e) with (g), we can see that the transmitter module modulates the transmitted signal to the transmission frequency 300 MHz, and we can find the AWGN is added in the received signal by comparing fig. 5.11 (g) with (i). The receiver module moves the received signal frequency back to baseband. Fig. 5.11 (b) and (c) show that the signal is recovered at the receiver even when AWGN exist, which means that all the modules in this simulation model work well.

5.1.3 Frequency-hopping spread spectrum

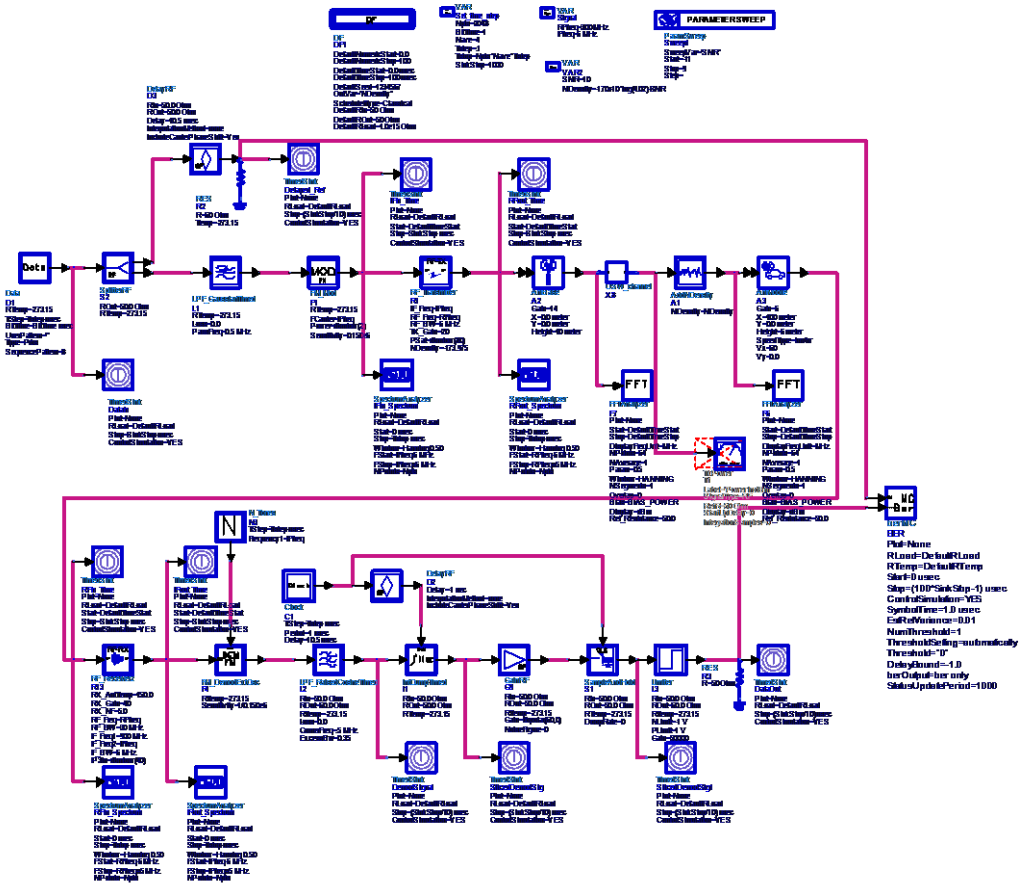

Fig. 5.12 FHSS simulation model

The work principle of the FHSS simulation model is shown in Fig. 5.12, which is composed by the modules we built in section 5.1.1. This simulation model realizes frequency-hopping, and the FSK module replaces the hopping module to achieve the frequency-hopping function. The transmitter modulates the transmitted signal to ultra-short wave spectrum 300 MHz. Then we can get the following figures after simulation.

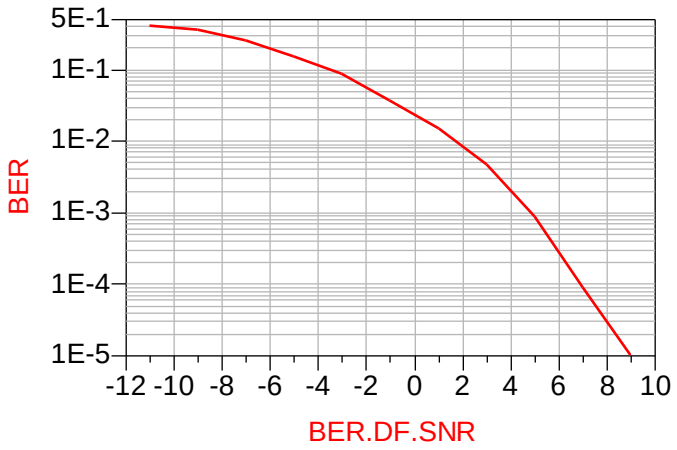

(a) BER of FHSS

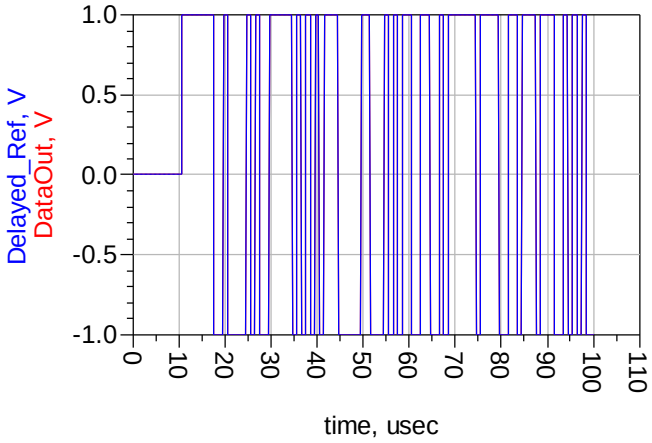

(b) time domain waveform of input and output

Fig. 5.13 simulation results of FHSS

We can see from fig. 5.13 (a) that the BER decreases with the increase of SNR, and this system is good at resisting the AWGN. Fig. 5.13 (b) shows that the signal is recovered at the receiver even when AWGN exist, which means that all the modules in this simulation model work well.

5.2 Matlab/Simulink simulation

DSSS and FHSS modules can't be integrated into a system in ADS, but it can be realized in Simulink. Simulink is better at processing digital signals than ADS. So the main simulation works are done in Simulink.

5.2.1 Channel coding

The channel coding technologies we used in SPCS are cyclic redundancy check (CRC), Reed-Solomon (RS) codes and interleaving. Fig. 5.14 shows the channel coding model, which includes general CRC generator, matlab function, bit to integer converter, integer-input RS encoder, general block interleaver and integer to bit converter. The channel coding model is packaged into a module named 'coder'. We will use the module 'coder' in the following section.

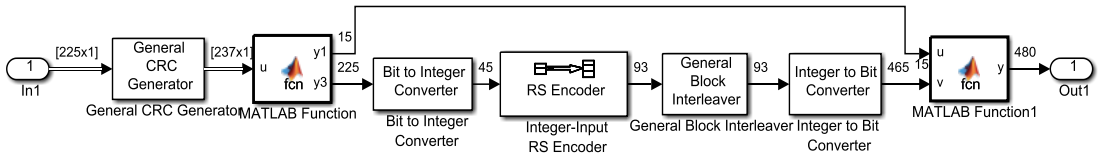

Fig. 5.14 channel coding model

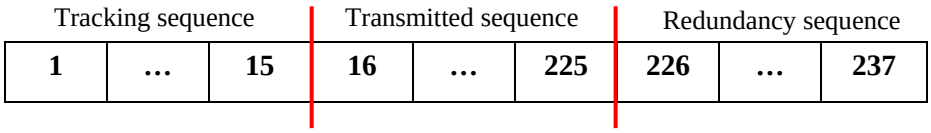

Fig. 5.15 data after CRC (237, 225)

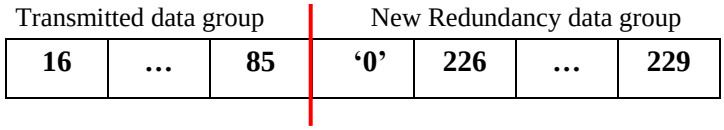

Fig. 5.16 one group after 'Matlab Function'

The input frame is 225 bits, which consists of 15 bits tracking sequence and 210 bits transmitted sequence. Every frame of general CRC generator's input data is 225 bits, and the output frame is 237 bits because CRC (237, 225) is used. The 12 bits redundancy sequence is added after the input frame. And the 12 bits redundancy sequence is divided into 3 groups, and each group is 4 bits. Padding one '0' at the beginning of each group, then each new group is 5 bits. The transmitted sequence of 210 bits is divided into 3 groups too, and each group is

70 bits. Joint each transmitted sequence consists of 70 bits and each redundancy sequence 5 bits to form the group of 75 bits. Then we link all 3 groups of 75 bits to form a 225 bits transmission data. So the input of bit to integer converter is 225 bits, and every 5 bits are converted into 1 integer. The output of the converter is 45 integers. The parameters of the integer-input RS encoder we set to RS (31, 15). The 45 integers are divided into 3 groups, and each group is 15 integers, 15 integers input and 31 integers output from integer-input RS encoder module. So every frame output of integer-input RS encoder is 3 groups, and each group is 31 integers. The schematic diagram of the general block interleaver module is shown in fig. 5.17, with input data inserted to rows, and output data read from columns. Now the interleaver module transfers the burst interference to be random interference, and divides the errors into each group to make the RS codes play the biggest role. Then the integer to bit converter module converts each integer back to 5 bits and 465 bits in total. [12]

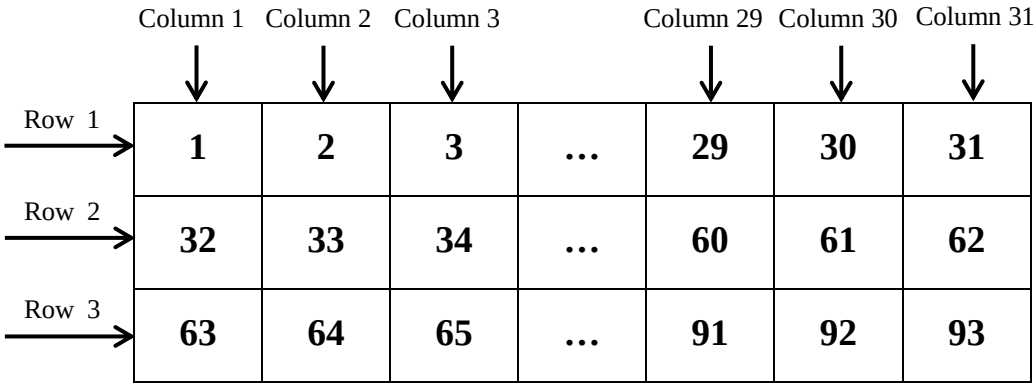

Fig 5.17 schematic diagram of interleaving

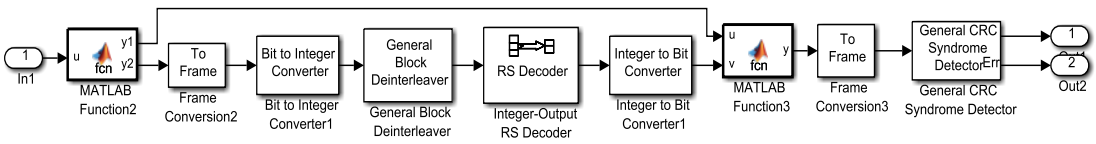

Fig. 5.18 channel decoding model

Fig. 5.18 shows channel decoding model, which includes matlab function, bit to integer converter, general block deinterleaver, integer-input RS decoder, integer to bit converter and general CRC syndrome detector. The channel coding model is packaged into a module named ‘decoder’. We will also use the module ‘decoder’ in the following section. The channel decoding model is the back-up process of the channel coding model.

The Reed–Solomon code we used in our communication system is RS (31, 15). In order to estimate RS (31, 15) error correction performance, we build the simulation model below. The simulation model includes random integer generator, binary-input RS encoder, frame

conversion, binary symmetric channel, binary-output RS decoder, error rate calculation and SER display.

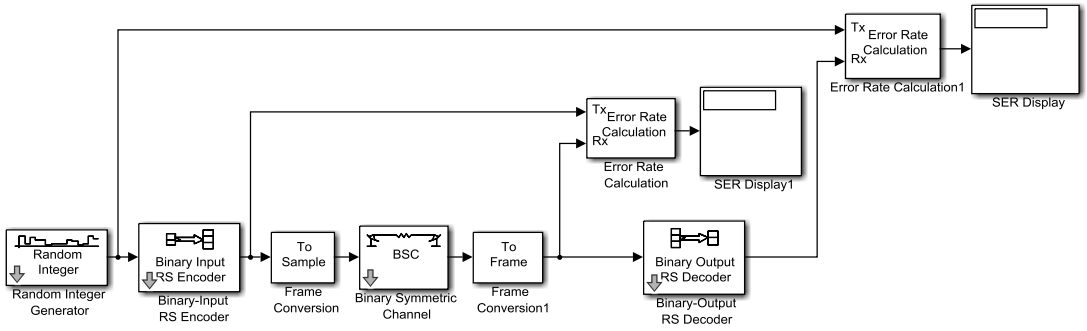

Fig. 5.19 RS (31, 15) simulation model

The figure above shows the RS (31, 15) error correction performance simulation model. The parameters of the model are set as follows: the sample time of random integer generator is 2e-6s and the codeword length and the message length of binary-input RS encoder are 31 and 15 respectively. The parameters of the binary-output RS encoder we set are the same as binary-input RS encoder. Then we change the parameter error probability of the binary symmetric channel to set different channel error probability. The simulation results are shown in the figure below.

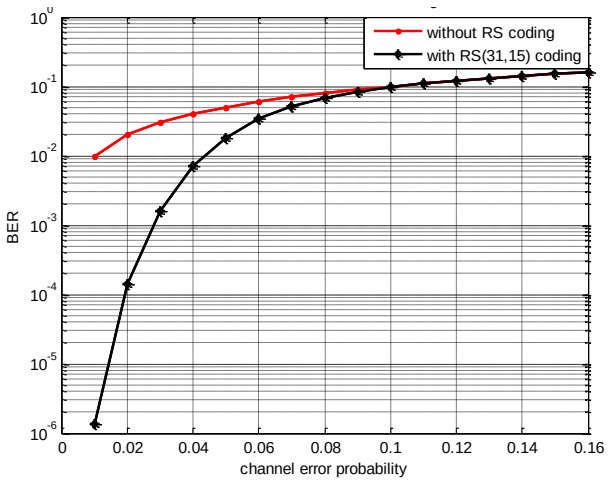

Fig. 5.20 BER of RS (31, 15)

Fig. 5.20 indicates the error correction performance of RS code is good. The higher SNR is, the better the RS code error correction performance. The reason is that there is an error correction threshold of RS codes. Once the number of errors is more than the error correction threshold, the RS codes will lose all the error correction ability. The worse channel, the bigger probability of the error number exceeds the error correction threshold. In this way, RS codes can't play a role. We can see from fig. 5.20 that the BER of the simulation model with and

without RS coding are 0.15e-6 and 0.01, respectively. The BER of the simulation model with RS coding is lower than that of the model without RS coding while the channel error probability is lower than 0.1. When the channel error probability is higher than 0.1, the BERs of the simulation model with and without RS coding are the same. It means that the number of errors exceeds the error correction threshold, and the RS code doesn't play a role.

5.2.2 BPSK modulation

The modulation we used in our communication system is Binary Phase-shift keying (BPSK). In order to estimate BPSK modulation performance, we build the simulation model below. The simulation model includes a Bernoulli binary generator, BPSK modulation baseband, AWGN channel, BPSK demodulation baseband, error rate calculation and SER display.

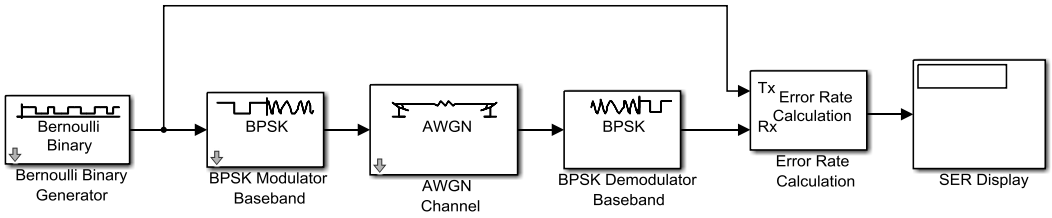

Fig. 5.21 BPSK modulation simulation model

The figure above shows the BPSK modulation simulation model. The parameters of the model are set as follows: the sample time of the Bernoulli binary generator is 2e-6s. Then we change the parameter signal to noise ratio of the AWGN channel to set different SNR (dB). The simulation results are shown in the figure below.

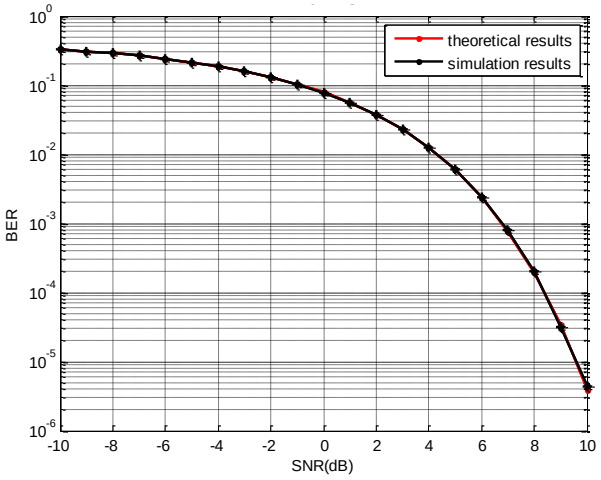

Fig. 5.22 BER of BPSK modulation

We can see from fig. 5.22 that the BERs of theoretical and simulation results are almost the same. It means that the BPSK modulation simulation model we used has good simulation accuracy characteristics. It can also make sure that the simulation results of the following sections are accurate.

5.2.3 Direct-sequence spread spectrum

The modeling principle of DSSS system is to make the sample rate of PN sequence generator be many times bigger than system transmission sample rate. In the simulation model below, the sample rate of the PN sequence generator is 10 times of the system transmission rate to realize 10 times spread spectrum. But two signals with different rate can't multiply together in Simulink. So we use a rate transition module to make the two signals' rate to be the same. Every data of system transmission sequence is repeated for 10 times to realize increasing the system transmission rate after the rate transition module. At the receiver, we do a 10 times downsample process to de-spread spectrum the signal.

The figure below shows the BPSK modulation DSSS simulation model. The simulation model includes a Bernoulli binary generator, unipolar to bipolar converter, rate transition, PN sequence generator, product, BPSK modulation baseband, AWGN channel, BPSK demodulation baseband, downsample, error rate calculation and SER display.

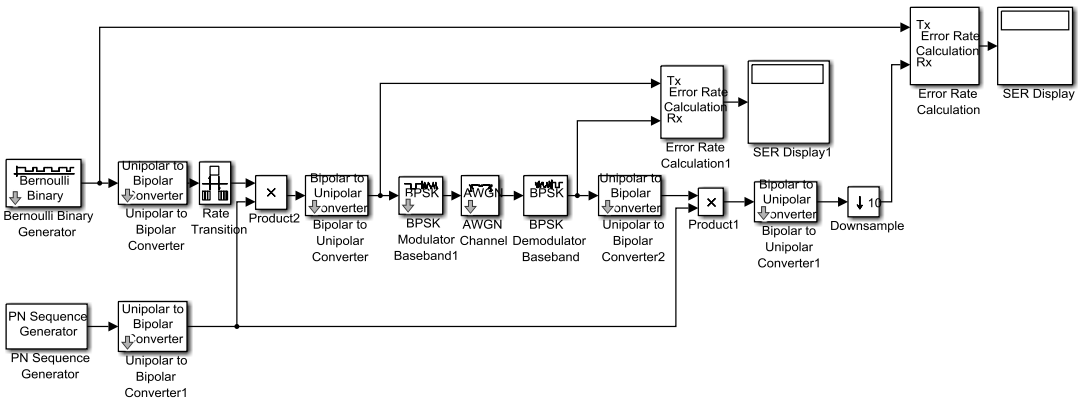

Fig. 5.23 BPSK modulation DSSS simulation model

The parameters of the above model are set as follows: the sample time of the Bernoulli binary generator and PN sequence generator are 1e-6s and 1e-7 respectively and the downsample factor is 10. Then we change the parameter signal to noise ratio of the AWGN channel to set different SNR (dB). The simulation results are shown as the figure below.

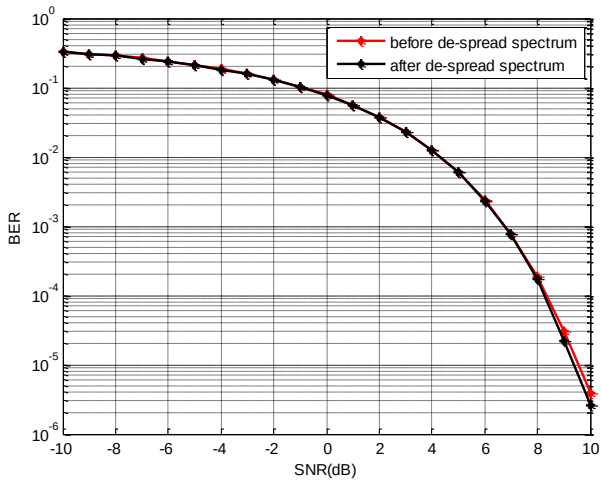

Fig. 5.24 BER of BPSK modulation DSSS

Fig. 5.24 shows that the ability to resist additive white Gaussian noise is good. The BER curve in fig. 5.24 is similar to the BER curve in fig. 5.11 (a) simulated by the software ADS, which indicates that the accuracy of these simulation results is good. And we also can see from this figure that the BER curves with and without the DSSS module are almost the same. This is because the noise power suppression capability of the spread spectrum communication system is the ratio of spread spectrum bandwidth to the noise bandwidth, as we discussed in section 3.1.2. When the noise bandwidth and the spread spectrum bandwidth are both very wide, the noise power suppression ability of the system is no longer significant. The bandwidth of the AWGN channel module we used in Simulink is very wide.

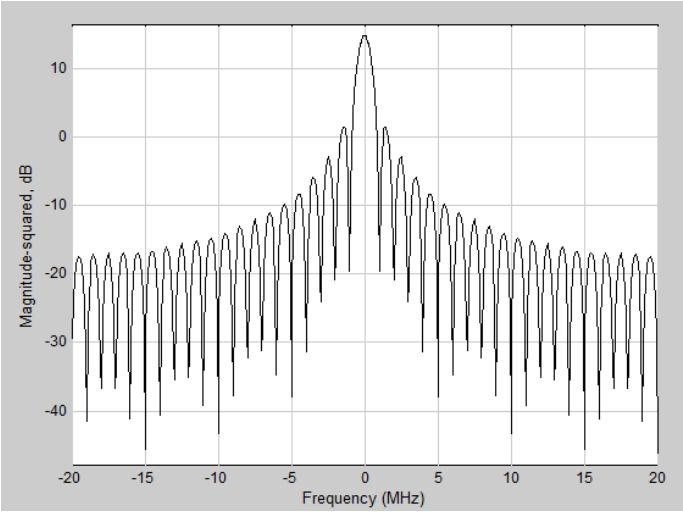

Fig. 5.25 frequency spectrogram before DSSS

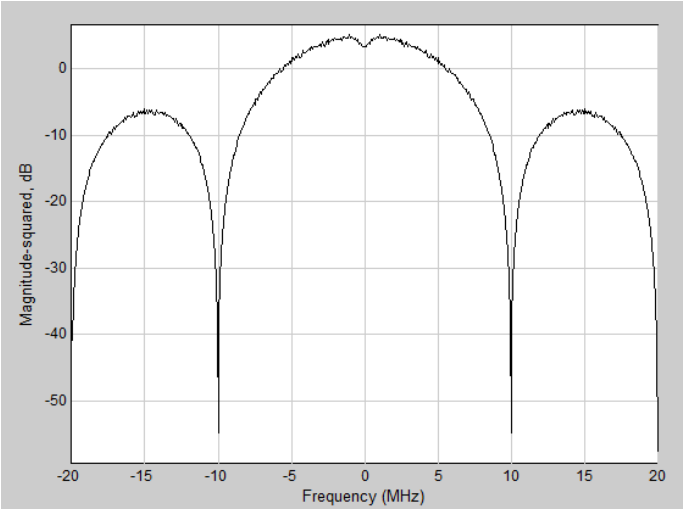

Fig. 5.26 frequency spectrogram after DSSS

Comparing fig. 5.25 with fig. 5.26, we can find that the bandwidth after DSSS is 10 times of the bandwidth before DSSS. The BPSK modulation DSSS simulation model we designed realizes 10 times spread spectrum, and the spreading gain is $10\log 10 = 10\,\text{dB}$. We can find that the amplitude after DSSS is 10 dB lower than the amplitude before DSSS. So the spread signal can be hidden in the noise to avoid being detected during the transmission.

5.2.4 Frequency-hopping spread spectrum

The modeling principle of frequency-hopping simulation system is the product of modulated signal and the certain frequency signal which is generated by FSK modulator baseband and PN sequence generator modules. The carrier frequency of the communication system is changing rapidly and randomly with the PN sequence to avoid single frequency and narrow bandwidth interferences.

The figure below shows the BPSK modulation frequency-hopping simulation model. The simulation model includes a Bernoulli binary generator, PN sequence generator, frame conversion, bit to integer conversion, M-FSK modulation baseband, product, BPSK modulation baseband, raised cosine filter, AWGN channel, BPSK demodulation baseband, downsample, error rate calculation and SER display.

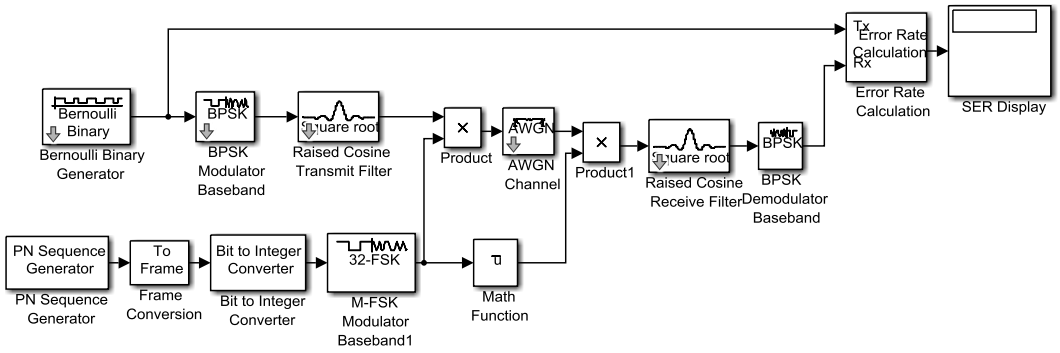

Fig. 5.27 BPSK modulation frequency-hopping simulation model

The parameters of the above model are set as follows: the sample time of the Bernoulli binary generator and PN sequence generator are 1e-6s and 0.2e-6 respectively. Every five bits of the PN sequence are converted to an integer to be the input of M-FSK modulation baseband module. Then the rates of system transmission and the hopping signal are the same, so it is an equal speed frequency-hopping system. The frequency separation of M-FSK modulation baseband module is 1 MHz, and M-ary number is 32. Based on the chosen parameters, the working frequency of this frequency-hopping system can hop among 32 frequency points, and the frequency separation of every two neighbouring frequency points is 1 MHz. We add a single frequency interference signal to this BPSK modulation frequency-hopping simulation model, and then it becomes the simulation model below.

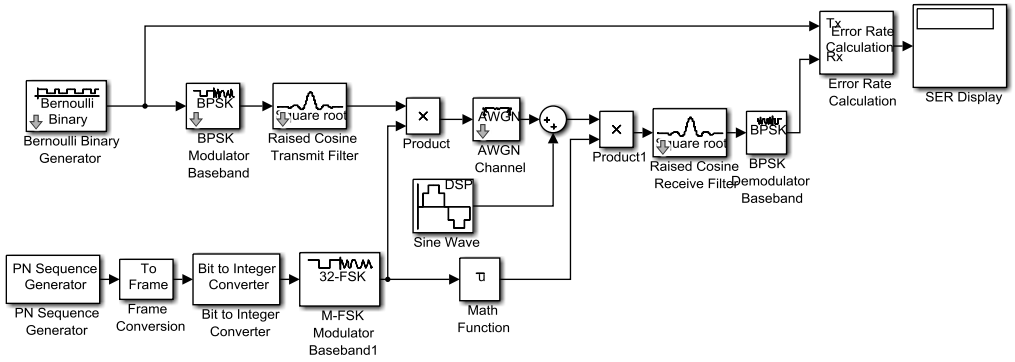

Fig. 5.28 BPSK modulation frequency-hopping simulation model (with single frequency interference)

Fig. 5.28 shows the BPSK modulation frequency-hopping simulation model with single frequency interference signal. All the parameters of this model are the same as the model shown in fig. 5.27. The only difference is that we added a single frequency interference signal here. The frequency of this single frequency interference signal is 10 KHz. The frequency spectrogram changing processes of this model are shown in the figures as follows.

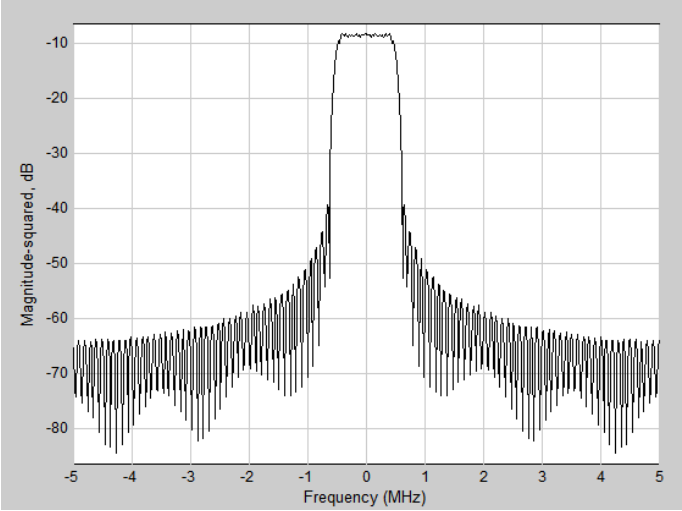

Fig. 5.29 frequency spectrogram after modulation

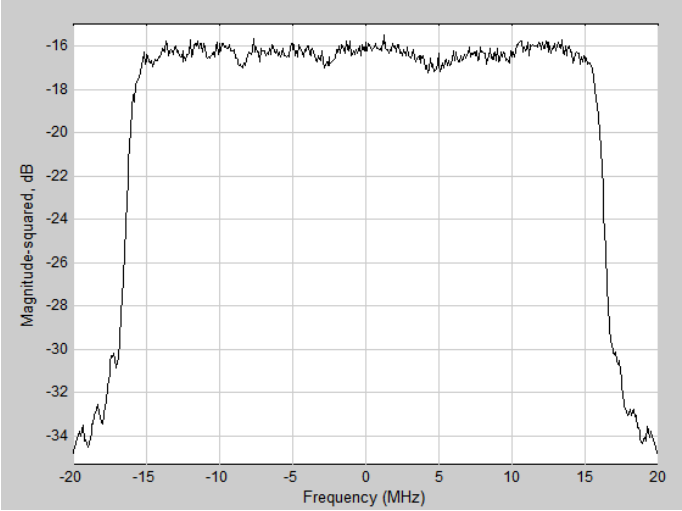

Fig. 5.30 frequency spectrogram after frequency-hopping

Comparing fig. 5.29 with fig. 5.30, we can see that the spectrum bandwidth is broadened obviously. There are 32 frequency points and the frequency separation is 1 MHz. And 32*1MHz=32 MHz. The bandwidth of the signal in fig. 5.30 is 32 MHz. So the frequency spectrogram result meets the system design requirement.

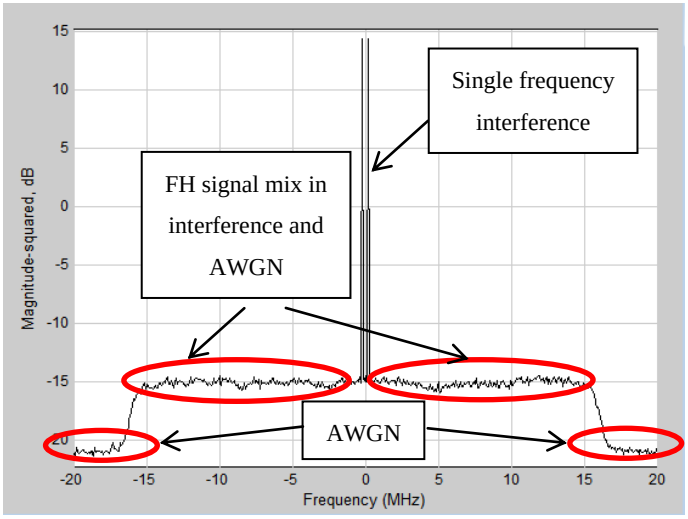

Fig. 5.31 frequency spectrogram after channel

Comparing fig. 5.30 with fig. 5.31, we can see that there is a single frequency interference signal in fig. 5.31. There are also some Gaussian white noise and frequency-hopping signals frequency spectrogram in fig. 5.31.

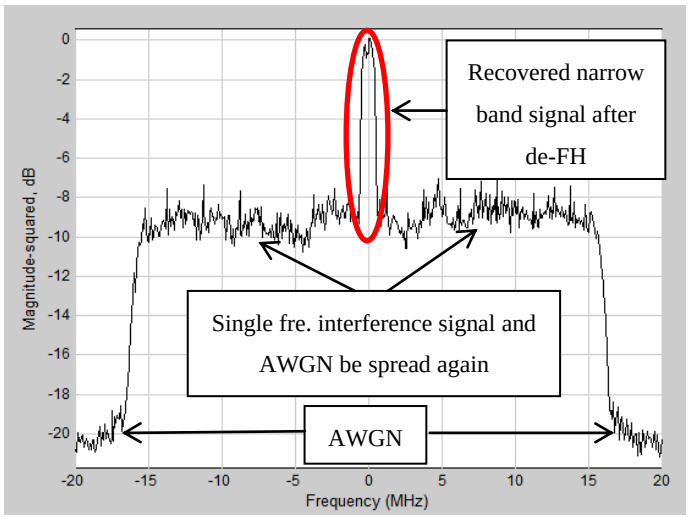

Fig. 5.32 frequency spectrogram after de-frequency-hopping

Fig. 5.32 is frequency spectrogram of the signal after de-frequency-hopping. The center narrow band part signal is high identical with the modulated signal in fig. 5.29. The frequency spectrum of single frequency interference and AWGN signal are spread again to the both sides of the recovered center narrow band signal. And the transmitted signals are recovered even single frequency interference signal exists.

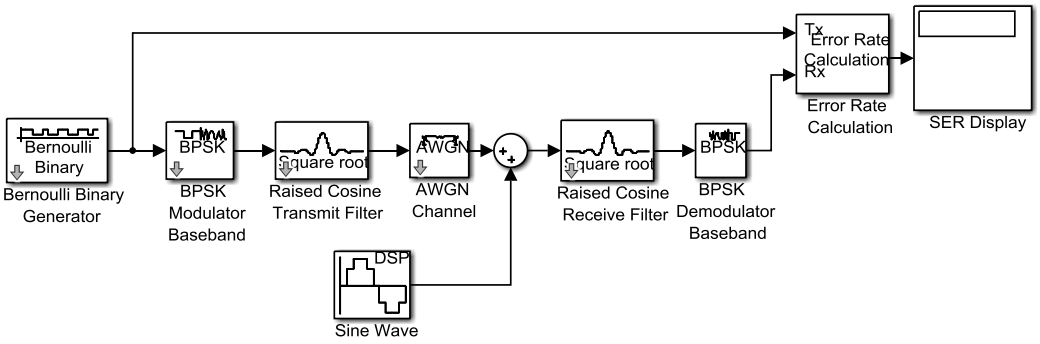

Fig. 5.33 BPSK modulation simulation model (with single frequency interference and without frequency-hopping)

We delete the frequency-hopping modules of fig. 5.28 to get the BPSK modulation simulation model in fig. 5.33. The remaining modules parameters in fig. 5.33 are the same with the modules parameters in fig. 5.28. Then we can get the BER figure below through changing the interference signal power.

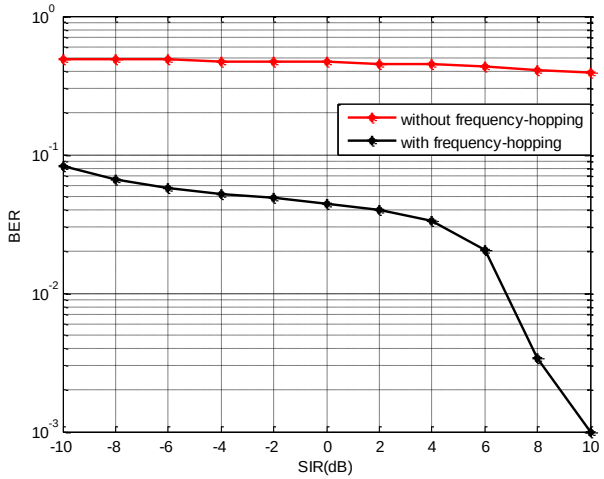

Fig. 5.34 BER of single frequency interference with and without frequency-hopping

Fig. 5.34 indicates the anti-jamming capability of single frequency interference of the system with and without frequency-hopping module. We can see from the fig. 5.34 that the BER of frequency-hopping system is much lower than the system without frequency-hopping module. Furthermore, the BER of the frequency-hopping system decreases while signal to interference ratio (SIR) increases. Instead, the BER of the no frequency-hopping system keeps unchanged on a high value while SIR increases. This means that the frequency-hopping system has a good ability to resist single frequency interference.

5.2.5 DSSS system

We add channel coding and decoding parts to the BPSK modulation DSSS simulation model in section 5.2.3 to build the simulation model below. Most parameters of this model are the same with the simulation model of section 5.2.3, but the sample time of the PN sequence generator should be (3e-6)/64s rather than 1e-7s. The output data of the channel coding module consists of many redundancy data generated in the channel coding module. The sample rate becomes (3e-5)/64s. Then we change the parameter signal to noise ratio of the AWGN channel to set different SNR (dB). The simulation results are shown in fig. 5.36. Some modules in the simulation model will cause delay. We should find out the accurate delay of the system, and then use the delay module to make sure the synchronization of received data and DSSS pseudorandom codes. The delay of the below simulation model is 10.

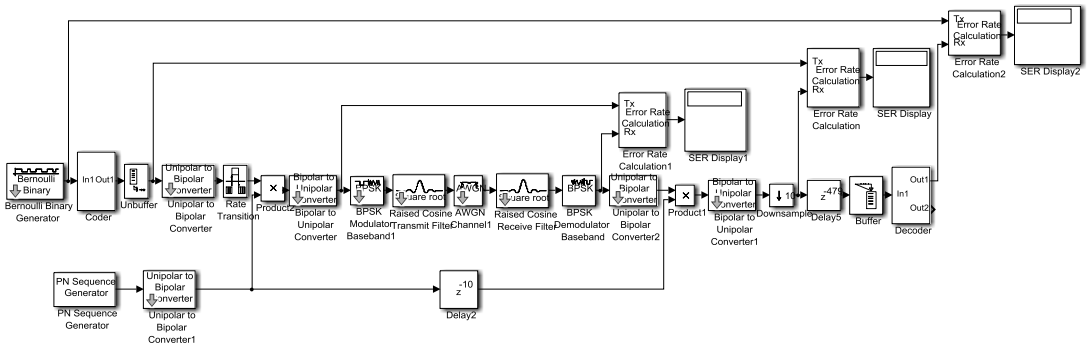

Fig. 5.35 BPSK modulation DSSS simulation model (with channel coding)

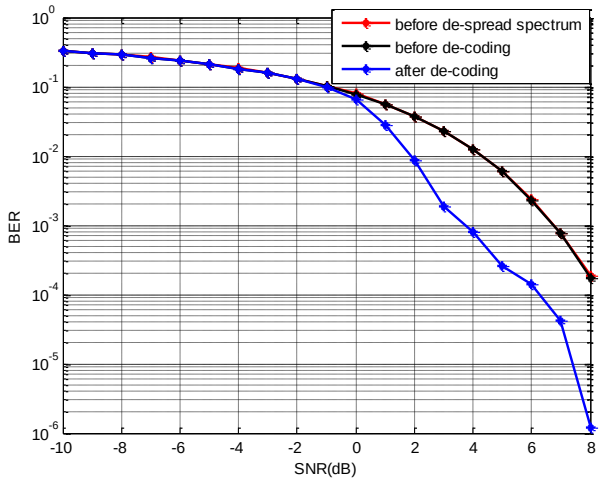

Fig. 5.36 BER of BPSK modulation DSSS simulation model (with channel coding)

We can see from fig. 5.36 the BER of the blue line is obviously lower than others when SNR is higher than -1 dB. This result illustrates that the channel coding and decoding parts can improve the system performance effectively.

5.2.6 DSSS and FHSS system

In this section, we add DSSS, FHSS and channel coding modules into one simulation model to build the SPCS.

The simulation model includes a Bernoulli binary generator, ‘coder’, unipolar to bipolar converter, rate transition, PN sequence generator, product, frame conversion, bit to integer conversion, M-FSK modulation baseband, product, BPSK modulation baseband, raised cosine filter, AWGN channel, BPSK demodulation baseband, downsample, error rate calculation and SER display.

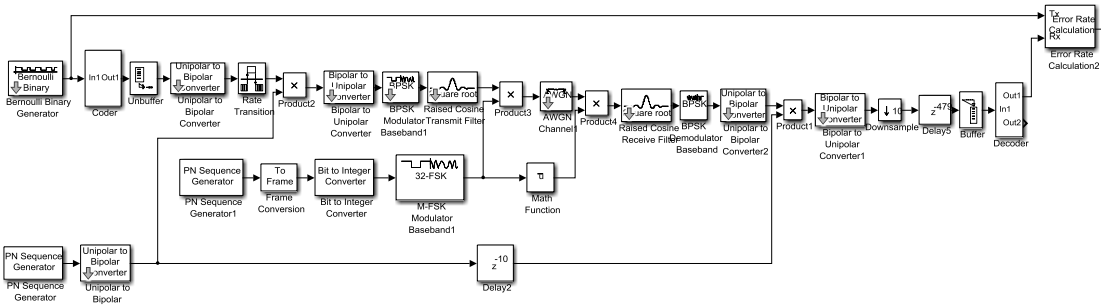

Fig. 5.37 BPSK modulation DSSS and FH simulation model (with channel coding)

The parameters of the above simulation model are set as follows: the sample time of the Bernoulli binary generator, PN sequence generator of FH model and PN sequence generator of DSSS model are 1e-6s, (3e-6)/64/5s, (3e-6)/64s respectively. The frequency separation of the M-FSK modulation baseband module is 10 MHz, and M-ary number is 32. Based on the chosen parameters, this system achieves 10 times DSSS. The working frequency of this frequency-hopping system can hop among 32 frequency points, and the frequency separation of every two neighbouring frequency points is 10 MHz. Then we change the parameter signal to noise ratio of the AWGN channel to set different SNR (dB). The simulation results are shown in fig. 5.38.

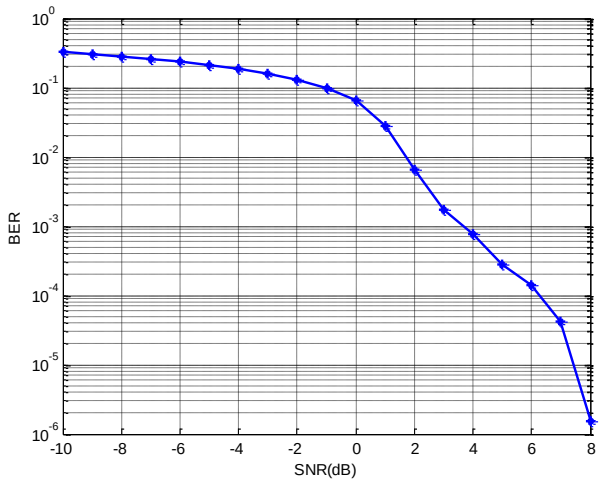

Fig. 5.38 BER of BPSK modulation DSSS and FH simulation model (with channel coding)

We can see from fig. 5.38 that the BPSK modulation DSSS and FH system also has a good capacity of resisting AWGN.

Then we add different kinds of EMI signals to the BPSK modulation DSSS and FHSS simulation model, and we get the figure of BER-SIR by adjusting the interference signal power. Here we will show the system frequency spectrogram changing processes as an example by using the noise amplitude modulation jamming signal.

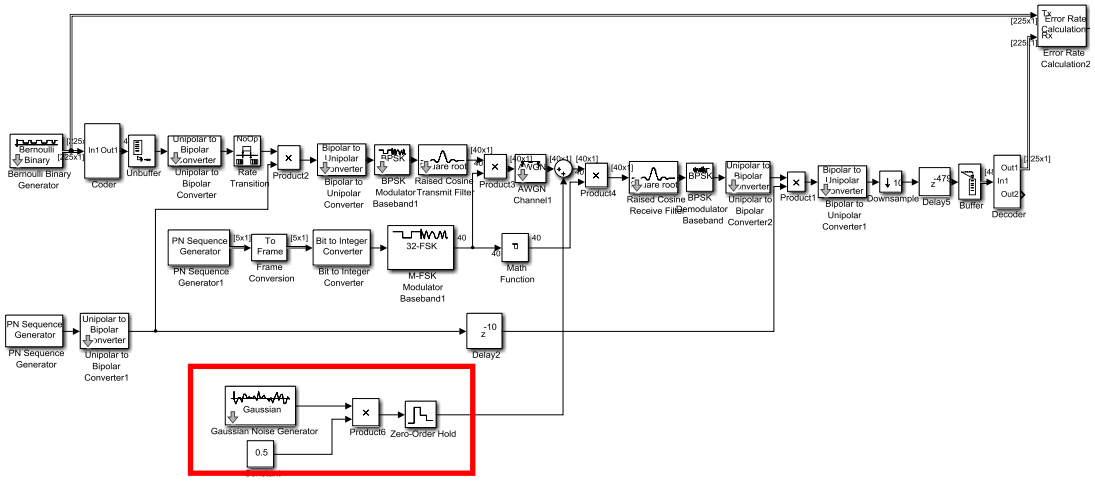

Fig. 5.39 BPSK modulation DSSS and FHSS resisting interference simulation model

All the parameters of this model are the same with the simulation model in fig. 5.37. The only difference is the jamming signal marked in red block that was added in this simulation model. The frequency spectrogram changing processes are shown from fig. 5.40 to fig. 5. 47.

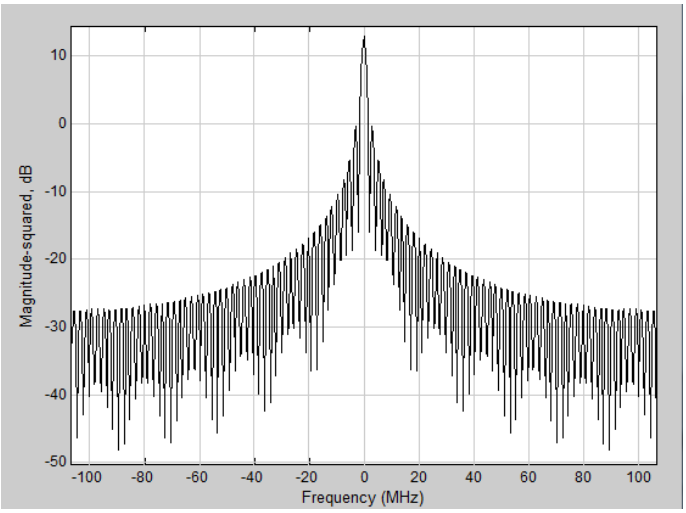

Fig. 5.40 frequency spectrogram after channel coding

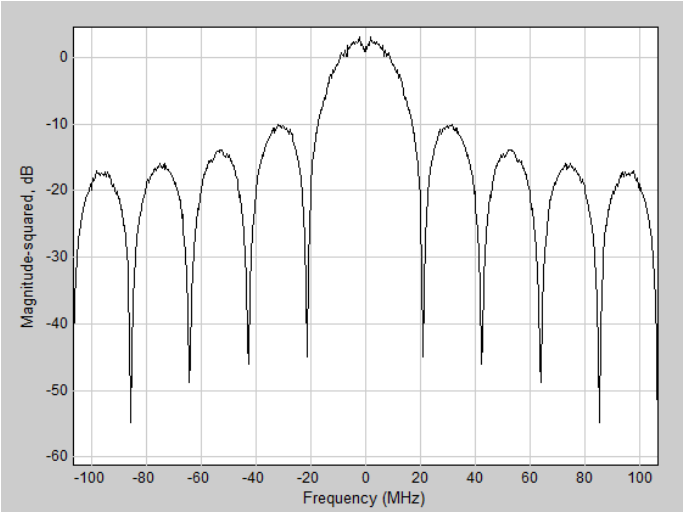

Fig. 5.41 frequency spectrogram after DSSS

Comparing fig. 5.40 with fig. 5.41, we can find that the bandwidth after DSSS is 10 times of the bandwidth before DSSS. The BPSK modulation DSSS simulation model we designed realizes 10 times spread spectrum.

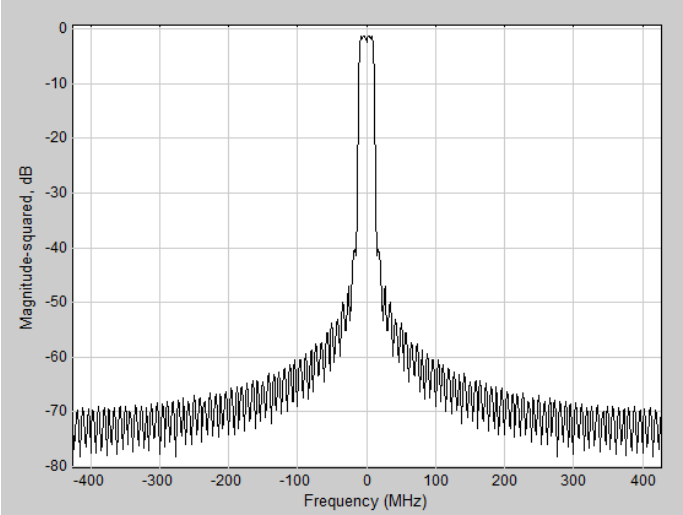

Fig. 5.42 frequency spectrogram after modulation

Fig. 5.42 is frequency spectrogram after modulation.

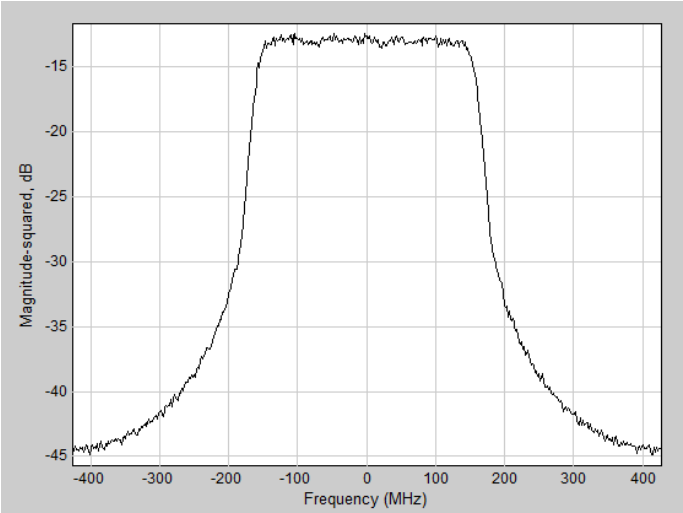

Fig. 5.43 frequency spectrogram after frequency-hopping

Comparing fig. 5.42 with fig. 5.43, we can see that the spectrum bandwidth is broadened obviously. There are 32 frequency points and the frequency separation is 10 MHz. And 32*10MHz=320 MHz. The bandwidth of the signal in fig. 5.43 is 320 MHz. So the frequency spectrogram result meets the system design requirement.

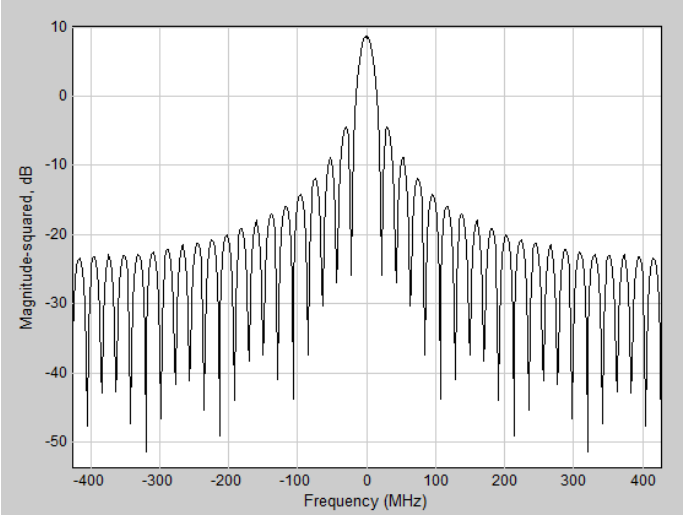

Fig. 5.44 frequency spectrogram of jamming signal

Fig. 5.44 is frequency spectrogram of jamming signal. The bandwidth of this jamming signal is a little wider that the modulated signal. Then we add the jamming signal to the spread transmission signal.

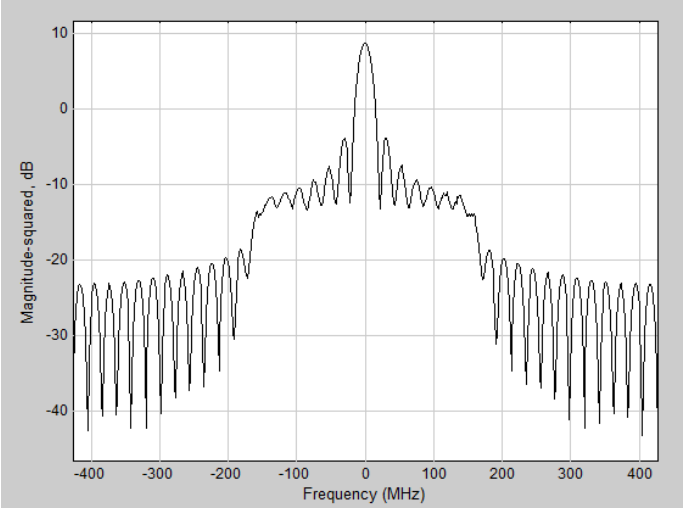

Fig. 5.45 frequency spectrogram of after channel

Fig. 5.45 is frequency spectrogram of after channel, and the jamming signal is added. We can see the signal is distorted by comparing fig.5.43 and fig.5.45.

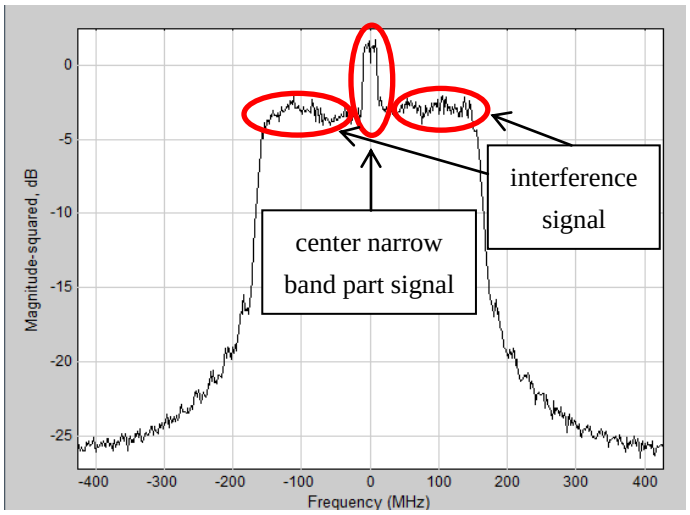

Fig. 5.46 frequency spectrogram after de-FHSS

Fig. 5.46 is frequency spectrogram after de-FHSS. The center narrow band part signal is highly identical with the modulated signal in fig. 5.42. It indicates that the modulated signal is recovered even when the transmission signal is distorted by the jamming signal seriously. The interference signal is spread again, which is moved to the both sides of the center useful signal after the de-frequency-hopping. And we can also find that there is AWGN effects in fig. 5.46 by comparing fig. 5.43 and fig. 5.46. Because we set the SNR(dB) of AWGN to be 100 dB in order to ignore the AWGN influence and only consider the influence of interference signal.

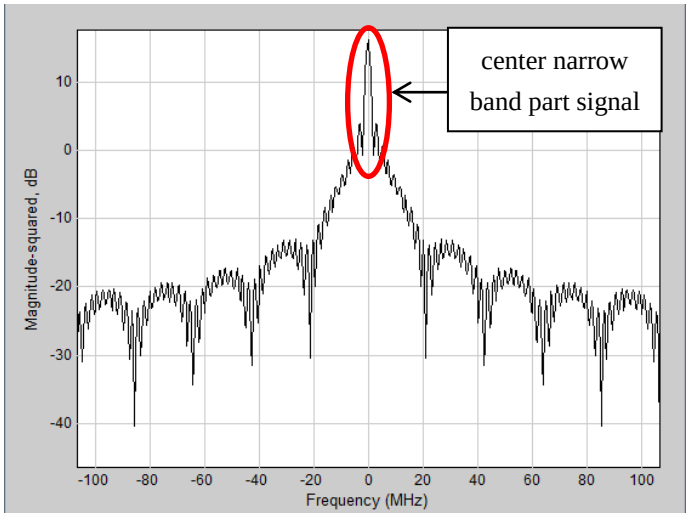

Fig. 5.47 frequency spectrogram after de-DSSS

Fig. 5.47 is frequency spectrogram after de-DSSS. The center narrow band part signal is highly identical with the signal after channel coding in fig. 5.40. It indicates that the

modulated signal is recovered even when the transmission signal is distorted by the jamming signal seriously.

From fig. 5.40 to fig.5.47, we can find that the main transmitted signal is recovered even when the EMI signal exists.

We can get the BER curves by changing the jamming signal type and adjusting the jamming signal power. In order to ignore the influence of AWGN and only consider the jamming influence, we set the parameter SNR of the AWGN channel module to be 100 dB. Adjusting the jamming signal power, we can get the simulation results below.

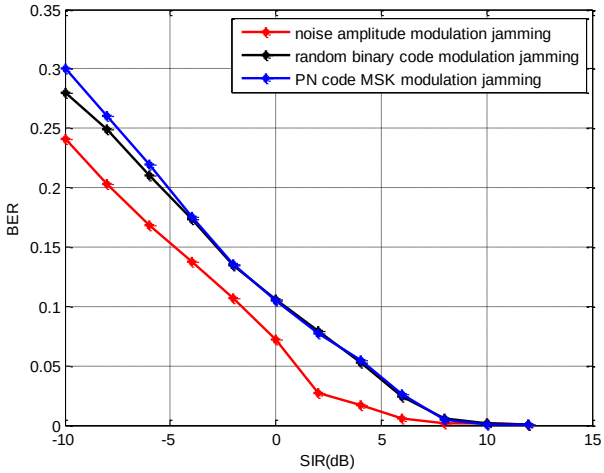

Fig. 5.48 BER of BPSK modulation DSSS and FH resisting different interferences simulation model

Fig. 5.48 is the BPSK modulation DSSS and FH system BER curves of noise amplitude modulation jamming, random binary code modulation jamming and PN code MSK modulation jamming. We can see from fig. 5.48 that the BER decreases as the SIR increases. The effect of those jamming signals to this BPSK modulation DSSS and FH system in decreasing order is PN code MSK modulation jamming, random binary code modulation jamming, and noise amplitude modulation jamming. The jamming effect of the PN code MSK modulation jamming is better than the random binary code modulation jamming effect when SIR is lower than -3 dB. Their jamming effects are almost the same when SIR is higher than -3 dB.

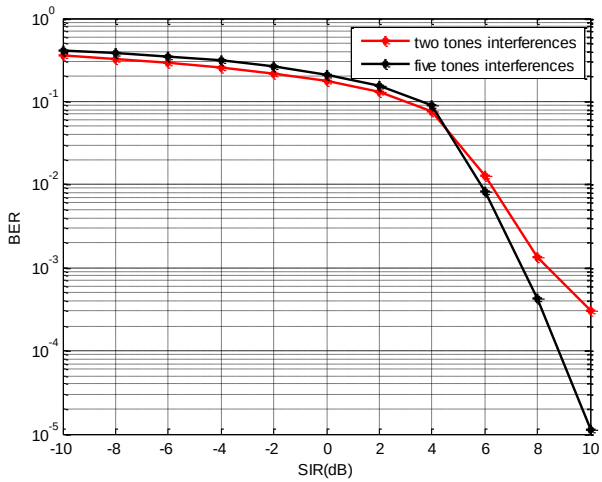

Fig. 5.49 BER of BPSK modulation DSSS and FH resisting different tone interferences simulation model

Fig. 5.49 is the BPSK modulation DSSS and FH system BER curves of two tones and five tones. The five tones are 10MHz and 70MHz and the seven tones are 10MHz、40MHz、70MHz、100MHz and 130MHz. We can see from fig. 5.49 that the jamming effect of five tones is better than two tones jamming effect when SIR is lower than 5 dB. This is because five tones jamming signal disturbs more frequency points on frequency domain. However, the jamming effect of five tones is worse than two tones jamming effect when SIR is higher than 5 dB. The reason is that each tone power of five tones jamming is smaller than the two tones jamming when the total jamming power is a constant. When the interference signal power is reduced to a certain extent, the interference power assigned to each frequency point is too small and the interference to the system is relatively small.

6 Conclusion

The aim of this thesis was to build up high-speed data link communication system model for ship platforms, with the help of some commercial software like MATLAB and ADS to further carry out simulation for predicting its system receiving characteristics; to explore some techniques to suppress EMI effects on the wireless communication performance. All of them have been accomplished.

The spread spectrum technologies of the SPCS consist of DSSS and FHSS were researched combined with spread spectrum theory. The channel coding techniques including CRC, RS codes and interleaving were introduced. The spread spectrum technologies and channel coding techniques were combined into an integrated communication system, and some EMIs were added into this communication system. The performance of the system can be summarized as follows:

(1) The channel coding model can decrease the BER of the system and improve the communication system performance effectively. There is an error correction threshold of the RS code. Once the number of errors is more than the error correction threshold, the RS code will lose all the error correction ability.
(2) The AWGN suppression capabilities of the communication system with and without DSSS module in simulation are almost the same. This is because the noise power suppression capability of the spread spectrum communication system is the ratio of spread spectrum bandwidth to the noise bandwidth. When the noise bandwidth and the spread spectrum bandwidth are both very wide, the noise power suppression ability of the system is no longer significant.
(3) The FHSS model has a very good ability of resisting single frequency interference.
(4) The communication system with DSSS module and FHSS model used together is good at resisting EMI effects.
(5) The effect of the jamming signals we built to the SPCS can be described as follows. The jamming effect of the PN code MSK modulation jamming is better than the random binary code modulation jamming effect, and the jamming effect of the noise amplitude modulation jamming is the worst.
(6) The jamming effect of five tones is better than that of two tones when SIR is small. While the jamming effect of five tones is worse than two tones jamming effect when SIR is big.

The simulation results we got are very significant to the practical design for the SPCS. But the channel of our simulation model is ideal, only considered the AWGN in the channel. In a future project, we should collect abundant transmission environment data of ships platform on the sea and build a channel simulation model for the sea transmission environment. Then we

should build the SPCS simulation model including the channel model. Under these circumstances, the simulation results would be more realistic.

Bibliography

[1] Kaur, M., Kakar, S., Mandal, D., Electromagnetic interference, Electronics Computer Technology, 3rd International Conference on 4 (2011) 1-5.

[2] Rong Hua, Chen Ming-Rong, Influence and Countermeasures on the Ship-borne Communication Equipment of Naval Field Complex Electromagnetic Environment , Distributed Computing and Applications to Business, Engineering & Science, 11th International Symposium on (2012) 345-347.

[3] R. L. Peterson, R.E. Ziemer, D.E. Borth, Introduction to Spread Spectrum Communications, Prentice-Hall, (1995).

[4] Logicon, Inc., Understanding Link 16: A Guidebook for New Users, San Diego, CA, (1994).

[5] Pickholtz, R.L., Schilling, D.L., Milstein, L.B., Theory of Spread-Spectrum Communications-A Tutorial, Communications, IEEE Transactions on 30 (5) 855-884.

[6] Hui Hu, Na Wei, A study of GPS jamming and anti-jamming, Power Electronics and Intelligent Transportation System (PEITS), 2nd International Conference on 1 (2009) 388 – 391.

[7] Upamanyu Madhow, Fundamentals of Digital Communication, Cambridge University Press, (2008).

[8] Michael B. Pursley, Direct-Sequence Spread-Spectrum Communications for Multipath Channels, Microwave Theory and Techniques, IEEE Transactions on 50 (3) (2012) 653-661.

[9] James H. Lindholm, An Analysis of the Pseudo-Randomness Properties of Subsequences of Long m-Sequences, Information theory, IEEE Transactions on l4 (4), (July 1968) 569-576.

[10] Pawula, R.F., Mathis, R.F., A Spread Spectrum System with Frequency Hopping and Sequentially Balanced Modulation--Part I: Basic Operation in Broadband Noise, Communications, IEEE Transactions on 28 (5) (May 1980) 682-688.

[11] Peterson, W. W. and Brown, D. T., Cyclic Codes for Error Detection, Proceedings of the IRE 49 (1) (Jan. 1961) 228–235.

[12] YIN Jun,YIN Ya-lan，XU Jian-zhong, Simulation Analysis of CRC-RS Coding in JTIDS, Communications Technology on 43 (5) (2010) 24-29.

[13] Reed, Irving S., Solomon, Gustave, Polynomial Codes over Certain Finite Fields, Journal of the Society for Industrial and Applied Mathematics (SIAM) 8 (2) (1960) 300–304.

[14] Chen, J., Owsley, P., A Burst-Error-Correcting Algorithm for Reed-Solomon Codes, Information Theory, IEEE Transactions on 38 (6) (Nov. 1992) 1807 – 1812.

[15]Branka Vucetic, Jinhong Yuan, Turbo Codes: Principles and Applications, Kluwer Academic, (June, 2000).

[16] J. B. Anderson, Digital Transmission Engineering , 2nd ed.,Wiley, (2005).

[17] H. Stern, S. Mahmoud, Communications Systems, Pearson Prentice Hall, (2004).

[18] R. A. Poisel, Modern Communications Jamming Principles and Techniques, Norwood: Artech House, (2004).

[19] Wang Hang, Wang Zanji , Guo Jingbo, Performance of DSSS against Repeater Jamming, Electronics, Circuits and Systems,13th IEEE International Conference on (Dec. 2006) 858-861.

[20] Albertson, R.T., Arthur, J., Rashid, M.H., Overview of Electromagnetic Interference, Power Symposium, NAPS 2006. 38th North American (Sept. 2006) 263 – 266.

[21] BlueTooth Simulation Example embedded in ADS software, path: C:\ADS2009U1\examples \Com_Sys\BlueTooth_prj.

[22] WIKIPEDIA. (n.d.). Reed–Solomon error correction. Retrieved from WIKIPEDIA: http://en.wikipedia.org/wiki/Reed%E2%80%93Solomon_error_correction#CITEREFWelch 1997.